J. Fluid Mech. (1978), *vol.* 85, *part* 1, *pp.* 97–142
Printed in Great Britain

The multiple-scale cumulant expansion for isotropic turbulence

By TOMOMASA TATSUMI,
Department of Physics, Faculty of Science, University of Kyoto, Kyoto 606, Japan
SHIGEO KIDA
Research Institute for Mathematical Sciences, University of Kyoto, Kyoto 606, Japan
AND JIRO MIZUSHIMA
Department of Physics, Faculty of Science, University of Kyoto, Kyoto 606, Japan†

(Received 10 August 1976 and in revised form 17 May 1977)

A method of multiple-scale expansion is applied to the theory of incompressible isotropic turbulence in order to close the infinite system of cumulant equations. The dynamical equation for the energy spectrum derived from this method is found to give positive-definite solutions at all Reynolds numbers. At large Reynolds numbers the spectrum takes the form of Kolmogorov's $-\frac{5}{3}$ power spectrum in the inertial subrange, whose extent increases indefinitely with Reynolds number. The spectrum in the energy-containing range satisfies an inviscid similarity law, so that the rate of energy decay or of viscous dissipation is also independent of the viscosity. In the higher wavenumber region beyond the inertial subrange the spectrum takes a universal form which is independent of its structure at lower wavenumbers. The universal spectrum is composed of three different subspectra, which are, in order of increasing wavenumber, the $k^{-\frac{5}{3}}$ spectrum, the k^{-1} spectrum and the $\exp[-\sigma k^{1.5}]$ spectrum, σ being a constant. Various statistical quantities such as the energy, the skewness of the velocity derivative, the microscale and the microscale Reynolds number are calculated from the numerical data for the energy spectrum. Theoretical results are discussed in detail in comparison with experimental results.

1. Introduction

The statistical theory of turbulence can be formulated either in terms of the probability distribution functional of the random velocity field or in terms of an infinite set of the moments of various orders. The former approach leads to Hopf's (1952) equation for the characteristic functional while the latter approach gives an infinite sequence of moment equations each relating a moment of nth order, n being a positive integer, with those of $(n+1)$th order. At present no method of solving Hopf's functional equation directly is known, so that the only alternative seems to be to deal with the moment equations or, in practice, a finite subset of them. In this approach, however, we are confronted with a difficulty of indeterminacy since the number of unknown

† Present address: Department of Mathematical Engineering, Sagami Institute of Technology, Fujisawa 251, Japan.

moments always exceeds by one the number of equations. In order to avoid this indeterminacy, a hypothesis is usually introduced to close the system of equations.

One of the closure hypotheses proposed so far is the zero-fourth-order cumulant approximation, which was first introduced for turbulence by Millionshtchikov (1941) and formulated for homogeneous isotropic turbulence by Proudman & Reid (1954) and Tatsumi (1955, 1957). This hypothesis enables us to relate the fourth-order moment to the second-order ones as if for a joint normal probability distribution, and in this sense it is also called the quasi-normality hypothesis. Formally, this hypothesis is equivalent to the fourth-order approximation of the cumulant expansion or the logarithmic Taylor expansion of the characteristic functional. This expansion seems to be a natural and logical approach to a random system which has nearly normal structure as a whole. There is also experimental evidence for this hypothesis as the measured two-point fourth-order moments and second-order moments satisfy the above relation very closely (Uberoi 1953; Frenkiel & Klebanoff 1967; Van Atta & Chen 1968, 1969; Van Atta & Yeh 1970).

In homogeneous isotropic turbulence, when the moment equations have been closed by this hypothesis they can be written in the form of a dynamical equation for the energy spectrum function $E(k,t)$, where k is the wavenumber and t the time. For extremely large values of the Reynolds number $R = u_0/(\nu k_0)$, u_0 and k_0 being a representative velocity and wavenumber of the turbulence respectively and ν the kinematic viscosity, the energy spectrum equation gives the following asymptotic solutions for different ranges of time (Tatsumi 1960):

$$E(k,t) \propto \begin{cases} k^{-2} & \text{for} \quad \tau = \nu k_0^2 t \ll 1, \qquad (1.1) \\ k^{-1} & \text{for} \quad \tau = \nu k_0^2 t \gg 1. \qquad (1.2) \end{cases}$$

It may be interesting to compare these asymptotic spectra with Kolmogorov's inertial-subrange spectrum

$$E(k,t) = K\epsilon^{\frac{2}{3}}k^{-\frac{5}{3}}, \qquad (1.3)$$

where ϵ is the rate of energy dissipation and K a non-dimensional constant (Kolmogorov 1941*a*, *c*). Neither (1.1) nor (1.2) is exactly in accordance with Kolmogorov's spectrum (1.3), but their exponents -1 and -2 bracket Kolmogorov's value $-\frac{5}{3}$.

However, unphysical consequences of this hypothesis were discovered by Ogura (1963), who found through numerical integration of the energy spectrum equation that the spectrum takes negative values over a finite range of wavenumbers at large Reynolds numbers. The occurrence of the negative spectrum gives rise to oscillation and eventual divergence of the solution, and therefore the asymptotic spectrum (1.2) is not attainable at least from the initial conditions adopted by Ogura. Such a consequence of the hypothesis seems to cast a serious doubt on its validity at large Reynolds numbers.

Thenceforth several attempts have been made to clarify the nature of this contradiction. Kawahara (1968) advanced the approximation a step further by working out the energy spectrum of Burgers turbulence under the zero-fifth-order cumulant approximation. It was found that the spectrum of this approximation still takes negative values at large Reynolds numbers, but it does so at higher wavenumbers and larger Reynolds numbers than those corresponding to the zero-fourth-order cumulant approximation. A similar trend in the solution was also observed by Tanaka (1969, 1973), who calculated numerically the energy spectrum of inviscid Burgers turbulence

using the zero-fifth-order cumulant approximation and the Gram–Charlier expansion truncated at various orders. The occurrence of the negative spectrum is not excluded by any approximations examined, but the wavenumber of first appearance of negative values becomes higher for a higher order of approximation and the spectrum in the energy-containing range of wavenumbers seems to converge to a limiting spectrum as the order of approximation increases. Thus it may be concluded from these results that a simple truncation of the cumulant expansion or the Gram–Charlier expansion cannot lead to a positive-definitive energy spectrum although it gives a good approximation in the lower wavenumber region.

The physical reason for the failure of the zero-cumulant approximation in general was discussed in detail by Orszag (1970). He examined a model turbulence which obeys an inviscid truncated Navier–Stokes equation in which the viscosity ν is identically zero and the Fourier expansion of the turbulent velocity field is truncated at a certain highest wavenumber. Concerning this model it is shown that the *time reversibility* of the zero-cumulant equations is not compatible with the unidirectional approach to the equilibrium and the lack of the proper *relaxation time* in the equations is responsible for the undamped oscillation of the solution around the equilibrium state. The occurrence of the negative energy spectrum is accounted for as a manifestation of this more fundamental weakness of the zero-cumulant approximation. The same argument can be applied to real turbulence which is governed by the full Navier–Stokes equation provided that the energy is always contained in turbulent components of finite wavenumber. In such a case the energy dissipation should vanish in the inviscid limit and the above-mentioned weakness of the zero-cumulant approximation would also appear in real turbulence. This is indeed what we experienced with the ordinary zero-cumulant approximation in real turbulence.

In order to improve this weakness several authors introduced various forms of *eddy viscosity*, which represents the effect of nonlinear scrambling of eddies or turbulent components of different wavenumbers (Edwards 1964; Kraichnan 1964, 1971; Herring 1965, 1966; Leith 1971). In these theories, the viscous damping of the cumulants is assumed to vanish in the inviscid limit and, in order to avoid time reversibility and the lack of a relaxation time in this limit, an eddy viscosity supplements the molecular viscosity or, more specifically, the viscous damping of the third-order cumulant. For the consequences of this kind of approximation reference may be made to the above papers and a numerical study by Herring & Kraichnan (1972).

In the present work, we shall take an approach of a quite different nature. It is well known that in laminar flows at large Reynolds numbers the viscous effects are confined to vortex layers or filaments whose thickness or radius is proportional to $\nu^{\frac{1}{2}}$ (Saffman 1968). This flow structure results in finite energy dissipation in the limit of vanishing viscosity. Now we expect that this characteristic of laminar flows is also possessed by turbulent flows since a particular realization of a turbulent flow is nothing but a solution of the same equation as for laminar flows. Thus we postulate for turbulent flows that a finite energy dissipation persists in the limit of vanishing viscosity, i.e.

$$\epsilon > 0 \quad \text{for} \quad \nu \to 0. \tag{1.4}$$

This postulate is equivalent to assuming that

$$\epsilon \text{ is independent of } \nu \text{ for very small } \nu. \tag{1.5}$$

Independence of ϵ and ν is tacitly assumed by Kolmogorov (1941 *a*) in his first hypothesis of similarity that, for locally isotropic turbulence, the distribution functions of turbulent velocity are uniquely determined by ϵ and ν. Hence our postulate (1.4) has a common background with Kolmogorov's hypothesis, but we are not going to use this hypothesis itself.

It follows immediately from (1.4) that the energy spectrum, or the second-order cumulant, has finite viscous damping and consequently the characteristic length scale is proportional to $\nu^{\frac{1}{2}}$ since otherwise the energy dissipation ϵ would not be finite in the inviscid limit. However, this does not mean that the length scale of order $\nu^{\frac{1}{2}}$ is the smallest scale of the turbulence. In turbulent flows the stretching of vortex layers and filaments due to non-uniform convection is much more vigorous than in laminar flows and the reduction in layers' thickness and filaments' radius gives rise to the generation of smaller length scales of order less than $\nu^{\frac{1}{2}}$. In the framework of the cumulant expansion this phase of motion is represented by the nonlinear terms, or the third- and higher-order cumulants. Thus it seems natural to expect that the higher-order cumulants have smaller length scales of orders ν, $\nu^{\frac{3}{4}}$, ..., and consequently that they are subject to larger viscous damping than the second-order cumulant.

In this context it should be noted that Kolmogorov's similarity hypothesis leads to an internal length scale $l = (\nu^3/\epsilon)^{\frac{1}{4}}$, which is proportional to $\nu^{\frac{3}{4}}$ as $\nu \to 0$ if the postulate (1.5) is accepted. Then there may arise the question why turbulence should have $\nu^{\frac{3}{4}}$ rather than $\nu^{\frac{1}{2}}$ dependence for the length scale of the viscous effects. This question is expected to be answered within the framework of the present expansion, which uses a set of different length scales. In fact it is shown in § 7.2 below that the energy spectrum derived from our approximation scheme actually satisfies Kolmogorov's similarity law, with the length scale proportional to $\nu^{\frac{3}{4}}$.

Summing up the above arguments, it may be said that our approximation scheme is at least free from such defects of the zero-cumulant approximation as were pointed out by Orszag, and is based upon an entirely different physical idea from that of the eddy-viscosity theories which assume vanishing effects of the molecular viscosity in the inviscid limit.

Now let us turn to the mathematical side of our approximation scheme. Formally speaking, the failure of the zero-fourth-cumulant approximation is a special case of breakdown of a regular perturbation scheme caused by the growth of a secular term. So far a number of methods and techniques have been devised for resolving this difficulty, most of them being singular perturbation methods which use multiple length or time scales to describe the nonlinear phenomena in question. A typical example of this method is the multiple time scale expansion method, originally due to Bogoliubov (1962).

The idea of different characteristic scales is by no means new to the theory of turbulence. It is common practice to expand the velocity field of incompressible turbulence in three-dimensional Fourier series and associate a Fourier component of wavenumber $\mathbf{k}$ with an eddy motion of a length scale $2\pi/|\mathbf{k}|$. Each Fourier component or eddy motion is supposed to have its own characteristic time scale, and usually the shorter time scales are associated with the smaller eddy motions or the larger wavenumber components as in Kolmogorov's universal equilibrium theory. Thus turbulence as a whole is regarded as composed of an infinite number of component motions associated with different time and length scales.

The method of multiple time scales was first applied by Malfliet (1969) to Burgers turbulence together with the zero-fourth-order cumulant hypothesis and it was shown that the energy spectrum derived from this method is positive definite at all Reynolds numbers. This result appears to be very promising and worth further investigation.

The multiple-scale expansion of Malfliet has two peculiar features. First, the turbulent velocity field is not expanded in the usual Fourier series but in terms of solutions of the linearized equation. This procedure amounts to taking the function

$$F(k,t) = E(k,t)\exp[2\nu k^2 t],$$

instead of $E(k,t)$ itself, as the most slowly varying function in the multiple-time-scale expansion. In other words, the purely viscous spectrum $E(k,t) = E(k,0)\exp[-2\nu k^2 t]$ is taken as the first approximation in the expansion. This choice of the first approximation does not seem to be adequate for strong turbulence. The second feature of his expansion is that the expansion parameter is not a real small parameter like that in the kinetic theory of statistical mechanics but a formal parameter which is eventually taken to be unity.† This makes the physical interpretation of his expansion rather obscure.

If the method of multiple-scale expansion is to be applied to turbulence the expansion parameter should be obtained from the field of turbulence itself. As already seen above there really exists a small parameter $\nu^{\frac{1}{2}}$ for the length scale of the energy spectrum. In what follows a multiple-scale expansion is formulated using this parameter. In §§ 2 and 3 an infinite system of equations governing the cumulants of different orders is derived from the Hopf equation for the characteristic functional. In § 4 the method of multiple-scale expansion is applied to this system of cumulant equations to give a closed dynamical equation for the energy spectrum. The initial-value problems for this equation are solved numerically in § 5, and the numerical results concerning the energy spectrum, the energy, the skewness, the microscale and so on are examined and discussed in detail in §§ 6–9.

2. Equation for the characteristic functional

The motion of an incompressible viscous fluid is governed by the following equations of continuity and motion:

$$\operatorname{div}\mathbf{u} = 0, \tag{2.1}$$

$$\partial\mathbf{u}/\partial t - \nu\Delta\mathbf{u} = -\rho^{-1}\operatorname{grad} p - (\mathbf{u}.\operatorname{grad})\mathbf{u}, \tag{2.2}$$

where $\mathbf{u} = \mathbf{u}(\mathbf{x},t)$ denotes the velocity, $p = p(\mathbf{x},t)$ the pressure, $\mathbf{x}$ the Cartesian coordinates, t the time, ρ the density and ν the kinematic viscosity of the fluid.

It is common practice in the theory of turbulence to introduce the Fourier transform of $\mathbf{u}(\mathbf{x},t)$:

$$\mathbf{v}(\mathbf{k},t) = (2\pi)^{-3}\int \mathbf{u}(\mathbf{x},t)\exp[-i\mathbf{k}.\mathbf{x}]\,d\mathbf{x}, \tag{2.3}$$

where $\mathbf{k}$ is the wavenumber vector and the integration is taken over the whole infinite space. For homogeneous turbulence, with which we are concerned, the right-hand side of (2.3) represents a divergent integral since $\mathbf{u}(\mathbf{x},t)$ does not vanish for $|\mathbf{x}|\to\infty$,

† Malfliet suggests the possibility of taking ν^2 as the small parameter. This choice, however, leads to inconsistent ordering of higher-order moments.

so that $\mathbf{v}(\mathbf{k},t)$ should be understood as a generalized function. Since the velocity $\mathbf{u}(\mathbf{x},t)$ is real, $\mathbf{v}(\mathbf{k},t)$ is a complex-valued function satisfying the relation

$$\mathbf{v}(-\mathbf{k},t) = \mathbf{v}^*(\mathbf{k},t), \tag{2.4}$$

where the asterisk denotes the complex conjugate. The inverse Fourier transform of (2.3) gives

$$\mathbf{u}(\mathbf{x},t) = \int \mathbf{v}(\mathbf{k},t) \exp[i\mathbf{k}.\mathbf{x}]\, d\mathbf{k}. \tag{2.5}$$

Substitution from (2.5) into (2.1) gives the orthogonality condition

$$\mathbf{k}.\mathbf{v}(\mathbf{k},t) = 0. \tag{2.6}$$

Taking the Fourier transform of (2.2) and eliminating the pressure p by making use of (2.6), we obtain the following equation for $\mathbf{v}(\mathbf{k},t)$:

$$\left(\frac{\partial}{\partial t} + \nu k^2\right)\mathbf{v}(\mathbf{k},t) = -i\int (\mathbf{k}.\mathbf{v}(\mathbf{k}-\mathbf{k}',t))\left\{\mathbf{v}(\mathbf{k}',t) - \frac{\mathbf{k}}{k^2}(\mathbf{k}.\mathbf{v}(\mathbf{k}',t))\right\} d\mathbf{k}', \tag{2.7}$$

where $k = |\mathbf{k}|$.

Now we define the characteristic functional of the probability distribution of $\mathbf{v}(\mathbf{k},t)$. Let us denote by $\mathbf{z}(\mathbf{k})$ a complex-valued argument function satisfying the condition

$$\mathbf{z}(-\mathbf{k}) = \mathbf{z}^*(\mathbf{k}) \tag{2.8}$$

and vanishing sufficiently rapidly as $k \to \infty$ to make the real-valued integral

$$(\mathbf{z},\mathbf{v}) = \int \mathbf{z}(\mathbf{k}).\mathbf{v}^*(\mathbf{k},t)\, d\mathbf{k} \tag{2.9}$$

convergent. Then the characteristic functional is defined as

$$\Phi[\mathbf{z}(\mathbf{k}),t] = \langle \exp[i(\mathbf{z},\mathbf{v})]\rangle, \tag{2.10}$$

where the angle brackets indicate the average with respect to the probability distribution of the function $\mathbf{v}(\mathbf{k})$ at time t.

The equation for the characteristic functional $\Phi[\mathbf{z}(\mathbf{k}),t]$ is derived from the law of conservation of probability and (2.7) as

$$\frac{\partial \Phi}{\partial t} + \int k^2 z_i(\mathbf{k}) \frac{\delta \Phi}{\delta z_i(\mathbf{k})}\, d\mathbf{k} = \iint (k_k + k'_k)\, \Delta_{ij}(\mathbf{k}+\mathbf{k}')\, z_i(\mathbf{k}+\mathbf{k}') \frac{\delta^2 \Phi}{\delta z_k(\mathbf{k})\, \delta z_j(\mathbf{k}')}\, d\mathbf{k}\, d\mathbf{k}', \tag{2.11}$$

with

$$\Delta_{ij}(\mathbf{k}) = \delta_{ij} - k_i k_j / k^2, \tag{2.12}$$

where $\delta/\delta z_i(\mathbf{k})$ represents the functional derivative, the suffixes i, j and k denote the components of a vector, and the summation convention for repeated suffixes is used hereafter. Equation (2.11), which was first derived by Hopf (1952), constitutes the basic equation of homogeneous turbulence in an incompressible viscous fluid, from which all the equations for the single-time moments of different orders can be derived.

It should be noted that an arbitrary solution of (2.11) is not necessarily a characteristic functional, but in order that it is admitted as a characteristic functional it should be a continuous positive-definite functional satisfying the conditions

$$\Phi[0,t] = 1, \quad |\Phi[\mathbf{z}(\mathbf{k}),t]| \leqslant 1, \quad \Phi[-\mathbf{z}(\mathbf{k}),t] = \Phi^*[\mathbf{z}(\mathbf{k}),t]. \tag{2.13}$$

In homogeneous turbulence the probability distribution is invariant under an arbitrary parallel transformation of the co-ordinates $\mathbf{x}$, so that Φ must satisfy an additional condition which follows from (2.3), (2.9) and (2.10), i.e.

$$\Phi\{\exp[i\mathbf{a}.\mathbf{k}]\,\mathbf{z}(\mathbf{k}), t\} = \Phi[\mathbf{z}(\mathbf{k}), t] \tag{2.14}$$

for an arbitrary real constant vector $\mathbf{a}$.

3. Equations for the cumulants

The moments of the probability distribution of $\mathbf{v}(\mathbf{k})$ are defined as the coefficients $M^{(n)}$ of the following Taylor expansion of the characteristic functional:

$$\Phi[\mathbf{z}(\mathbf{k}), t] = 1 + \sum_{n=1}^{\infty} \frac{i^n}{n!} \int \dots \int M^{(n)}_{l_1 \dots l_n}(\mathbf{k}_1, \dots, \mathbf{k}_n; t) \times \delta(\mathbf{k}_1 + \dots + \mathbf{k}_n)\, z_{l_1}(\mathbf{k}_1) \dots z_{l_n}(\mathbf{k}_n)\, d\mathbf{k}_1 \dots d\mathbf{k}_n, \tag{3.1}$$

where the factor $\delta(\mathbf{k}_1 + \dots + \mathbf{k}_n)$ is required by the condition (2.14). Likewise, the cumulants are defined as the coefficients $C^{(n)}$ of the logarithmic Taylor expansion

$$\Phi[\mathbf{z}(\mathbf{k}), t] = \exp\left[\sum_{n=1}^{\infty} \frac{i^n}{n!} \int \dots \int C^{(n)}_{l_1 \dots l_n}(\mathbf{k}_1, \dots, \mathbf{k}_n; t) \times \delta(\mathbf{k}_1 + \dots + \mathbf{k}_n)\, z_{l_1}(\mathbf{k}_1) \dots z_{l_n}(\mathbf{k}_n)\, d\mathbf{k}_1 \dots d\mathbf{k}_n\right]. \tag{3.2}$$

Obviously, $M^{(n)}$ and $C^{(n)}$ are invariant under the simultaneous permutation of the suffixes $(l_1, \dots, l_n)$ and the arguments $(\mathbf{k}_1, \dots, \mathbf{k}_n)$ and, in accordance with (2.8) and (2.13), satisfy the relation

$$\begin{pmatrix} M^{(n)} \\ C^{(n)} \end{pmatrix}_{l_1 \dots l_n} (-\mathbf{k}_1, \dots, -\mathbf{k}_n; t) = \begin{pmatrix} M^{(n)*} \\ C^{(n)*} \end{pmatrix}_{l_1 \dots l_n} (\mathbf{k}_1, \dots, \mathbf{k}_n; t). \tag{3.3}$$

As may easily be seen from (2.10) and (3.1), the moments are related to the mean velocity products in the following manner:

$$\begin{aligned} \langle v^*_{l_1}(\mathbf{k}_1, t) \dots v^*_{l_n}(\mathbf{k}_n, t)\rangle &= i^{-n} \left[\frac{\delta^n \Phi}{\delta z_{l_1}(\mathbf{k}_1) \dots \delta z_{l_n}(\mathbf{k}_n)}\right]_{\mathbf{z}=0} \\ &= M^{(n)}_{l_1 \dots l_n}(\mathbf{k}_1, \dots, \mathbf{k}_n; t)\, \delta(\mathbf{k}_1 + \dots + \mathbf{k}_n). \end{aligned} \tag{3.4}$$

Likewise, it follows from (3.2) that

$$i^{-n} \left[\frac{\delta^n \log \Phi}{\delta z_{l_1}(\mathbf{k}_1) \dots \delta z_{l_n}(\mathbf{k}_n)}\right]_{\mathbf{z}=0} = C^{(n)}_{l_1 \dots l_n}(\mathbf{k}_1, \dots, \mathbf{k}_n; t)\, \delta(\mathbf{k}_1 + \dots + \mathbf{k}_n). \tag{3.5}$$

Thus a cumulant of any order can be expressed in terms of the mean velocity products using relations (3.4) and (3.5).

The equations for the cumulants are obtained by substituting the expansion (3.2) into (2.11) and equating coefficients of the same powers of the $z_l(\mathbf{k})$'s as follows:

$$\left(\frac{\partial}{\partial t}+\nu\sum_{m=1}^{n}k_m^2\right)C^{(n)}_{l_1\dots l_n}(\mathbf{k}_1,\dots,\mathbf{k}_n;t)=i\sum_{m=1}^{n}(k_m)_p\,\Delta_{l_m q}(\mathbf{k}_m)$$
$$\times\int C^{(n+1)}_{l_1\dots l_{m-1}pl_{m+1}\dots l_n q}(\mathbf{k}_1,\dots,\mathbf{k}_{m-1},\mathbf{k}_m-\mathbf{h},\mathbf{k}_{m+1},\dots,\mathbf{k}_n,\mathbf{h};t)\,d\mathbf{h}$$
$$-i\sum_{r=2}^{n-1}\frac{1}{(r-1)!\,(n-r+1)!}\sum_{[1,\dots,n]}\sum_{m=r}^{n}(k_m)_p\,\Delta_{l_m q}(\mathbf{k}_m)$$
$$\times C^{(r)}_{l_1\dots l_{r-1}q}\left(\mathbf{k}_1,\dots,\mathbf{k}_{r-1},-\sum_{s=1}^{r-1}\mathbf{k}_s\right)$$
$$\times C^{(n-r+1)}_{l_r\dots l_{m-1}pl_{m+1}\dots l_n}(\mathbf{k}_r,\dots,\mathbf{k}_{m-1},\mathbf{k}_m+\sum_{s=1}^{r-1}\mathbf{k}_s,\mathbf{k}_{m+1},\dots,\mathbf{k}_n;t) \tag{3.6}$$

with $\mathbf{k}_1+\mathbf{k}_2+\dots+\mathbf{k}_n=0$, where $k_m=|\mathbf{k}_m|$ and $\sum_{[1,\dots,n]}$ means the sum over all permutations of $(1,2,\dots,n)$.

Equations (3.6) for $n=2,3,\dots$ represent an infinite system of equations each relating the cumulant of nth order to those of lower orders and that of $(n+1)$th order. It is the presence of the $(n+1)$th order cumulant that makes this system of equations indeterminate since any finite subset of them curtailed at a certain order always involves one more unknown cumulant than the number of equations. An assumption usually introduced in this context to make the finite subset of equations determinate is simply to neglect the cumulant of highest, i.e. $(n+1)$th, order, and this is generally called the zero-cumulant hypothesis. As may easily be seen from (3.4) and (3.5), the cumulants of first, second and third order are identical to the mean velocity products of the corresponding order, so that the zero-cumulant hypothesis is meaningful at least for the fourth-order cumulant.

The zero-fourth-order cumulant hypothesis, which was put forward by Proudman & Reid (1954) and Tatsumi (1955, 1957), is to neglect the terms $C^{(4)}$ in the following pair of equations, which are equivalent to (3.6) for $n=2$ and 3:

$$\left\{\frac{\partial}{\partial t}+\nu(k^2+k'^2)\right\}C^{(2)}_{ij}(\mathbf{k},\mathbf{k}';t)=i\sum_{[\mathbf{k},\mathbf{k}']}^{[i,j]}k_p\,\Delta_{iq}(\mathbf{k})\int C^{(3)}_{pjq}(\mathbf{k}-\mathbf{h},\mathbf{k}',\mathbf{h};t)\,d\mathbf{h} \tag{3.7}$$

with $\mathbf{k}+\mathbf{k}'=0$ and

$$\left\{\frac{\partial}{\partial t}+\nu(k^2+k'^2+k''^2)\right\}C^{(3)}_{ijk}(\mathbf{k},\mathbf{k}',\mathbf{k}'';t)$$
$$=i\sum_{[\mathbf{k},\mathbf{k}',\mathbf{k}'']}^{[i,j,k]}k_p\,\Delta_{iq}(\mathbf{k})\left\{\frac{1}{2}\int C^{(4)}_{pjkq}(\mathbf{k}-\mathbf{h},\mathbf{k}',\mathbf{k}'',\mathbf{h};t)\,d\mathbf{h}-C^{(2)}_{pj}(-\mathbf{k}',\mathbf{k}';t)\,C^{(2)}_{kq}(\mathbf{k}'',-\mathbf{k}'';t)\right\} \tag{3.8}$$

with $\mathbf{k}+\mathbf{k}'+\mathbf{k}''=0$, where the summations are taken over all simultaneous permutations of (i,j,k) and $(\mathbf{k},\mathbf{k}',\mathbf{k}'')$. The pair of equations (3.7) and (3.8) with the terms $C^{(4)}$ omitted gives a deterministic equation for $C^{(2)}$ on elimination of $C^{(3)}$, and for isotropic turbulence this equation is written in the form of an equation for the energy spectrum function $E(k,t)$. A detailed discussion of the consequences of this equation and the nature of the basic hypothesis has already been made in § 1. In order to overcome the defects of the zero-fourth-order cumulant hypothesis the multiple-scale cumulant expansion is introduced in the next section.

4. Multiple-scale cumulant expansion

The cumulant expansion (3.2) of the characteristic functional represents an expansion in ascending powers of the turbulent velocity since the cumulant $C^{(n)}$ is related to the mean velocity products of the same order through relations (3.4) and (3.5). In non-dimensional form it can be written as a power series in the Reynolds number based on the turbulent velocity. Thus there is good reason to believe that the cumulant expansion may be useful for dealing with weak turbulence at small Reynolds numbers but may be inadequate for strong turbulence at large Reynolds numbers. The failure of the zero-fourth-order cumulant approximation seems to confirm this belief.

It should be noted, however, that the cumulant expansion itself should not necessarily be taken as an expansion in ascending powers of the Reynolds number. In fact, it will be shown below that the cumulant expansion can be transformed into an asymptotic expansion for extremely large Reynolds numbers if an appropriate ordering of the variables is made.

The first two cumulant equations (3.7) and (3.8) may be written symbolically as

$$(\partial/\partial t + \nu k^2)\, C^{(2)} = k \int C^{(3)} d\mathbf{h}, \tag{4.1}$$

$$(\partial/\partial t + \nu k^2)\, C^{(3)} = k \int C^{(4)} d\mathbf{h} + k C^{(2)} C^{(2)}, \tag{4.2}$$

where, for convenience, all the variables are regarded as non-dimensional and the viscosity ν as a non-dimensional parameter equivalent to the reciprocal of the Reynolds number.

The physical arguments can be made more conveniently in terms of the averaged cumulants, which are defined as follows:

$$\left.\begin{aligned} \bar{C}^{(2)} &= \int C^{(2)}(\mathbf{k})\, k^2\, d\sigma, \\ \bar{C}^{(3)} &= \iint C^{(3)}(\mathbf{k}, \mathbf{k}')\, k^2 k'^2\, d\sigma\, d\sigma', \\ \bar{C}^{(4)} &= \iiint C^{(4)}(\mathbf{k}, \mathbf{k}', \mathbf{k}'')\, k^2 k'^2 k''^2\, d\sigma\, d\sigma'\, d\sigma'', \end{aligned}\right\} \tag{4.3}$$

where the σ's denote the solid angles in wavenumber space.

In isotropic turbulence $C^{(2)}$ and $\bar{C}^{(2)}$ are expressed as

$$C_{ij}^{(2)}(\mathbf{k}, -\mathbf{k}; t) = \phi(k, t)\, \Delta_{ij}(\mathbf{k}), \tag{4.4}$$

$$\bar{C}_{ij}^{(2)}(k, t) = \tfrac{8}{3}\pi k^2 \phi(k, t)\, \delta_{ij}. \tag{4.5}$$

Using (2.5), (2.4) and (3.5), the energy of the turbulence per unit mass is expressed as

$$\begin{aligned} \mathscr{E}(t) = \tfrac{1}{2}\langle |\mathbf{u}(\mathbf{x}, t)|^2 \rangle &= \frac{1}{2} \int C_{ii}^{(2)}(\mathbf{k}, -\mathbf{k}; t)\, d\mathbf{k} = \frac{1}{2} \int_0^\infty \bar{C}_{ii}^{(2)}(k, t)\, dk \\ &= 4\pi \int_0^\infty \phi(k, t)\, k^2\, dk = \int_0^\infty E(k, t)\, dk, \end{aligned} \tag{4.6}$$

where

$$E(k, t) = 4\pi k^2 \phi(k, t) = \tfrac{1}{2} \bar{C}_{ii}^{(2)}(k, t). \tag{4.7}$$

The scalar function $\phi(k, t)$ is called the energy spectrum density and $E(k, t)$ the energy spectrum function.

In terms of these averaged cumulants the symbolic equations (4.1) and (4.2) are rewritten as

$$(\partial/\partial t + \nu k^2)\, \bar{C}^{(2)} = k \int \bar{C}^{(3)} dh, \tag{4.8}$$

$$(\partial/\partial t + \nu k^2)\, \bar{C}^{(3)} = k \int \bar{C}^{(4)} dh + k \bar{C}^{(2)} \bar{C}^{(2)}. \tag{4.9}$$

Now we proceed to the estimation of the order of magnitude of the variables. At an initial instant the turbulent fluid has a finite amount of energy per unit mass $\mathscr{E}(0)$. At this time the intensity $\bar{C}^{(2)}$ of the energy spectrum and the energy-containing wavenumbers, for which $\bar{C}^{(2)}$ has non-zero values, are both assumed to be of the order of unity.

The statistical state of turbulence changes in time. At large Reynolds numbers it soon assumes an asymptotic state in which postulate (1.4) or (1.5) is satisfied. In such a state, as described in § 1, the second-order cumulant has a length scale of order $\nu^{\frac{1}{2}}$ and the higher-order cumulants have smaller length scales. Then, if we introduce a set of multiple wavenumber scales

$$k_n = \nu^{\frac{1}{2}n} k, \quad n = 1, 2, \ldots, \tag{4.10}$$

it is natural to assume that the cumulants depend on the wavenumber scales (4.10) as follows:

$$\left.\begin{aligned} \bar{C}^{(2)}(k) &= \bar{C}^{(2)}(k_1), \\ \bar{C}^{(3)}(k) &= \bar{C}^{(3)}(k_1, k_2), \\ \bar{C}^{(4)}(k) &= \bar{C}^{(4)}(k_1, k_2, k_3), \quad \text{etc.} \end{aligned}\right\} \tag{4.11}$$

The variation of the cumulants in time is likewise expressed in terms of the multiple time scales

$$t_n = \nu^{-n} t, \quad n = 0, 1, 2, \ldots . \tag{4.12}$$

Then the time derivative is written as

$$\frac{\partial}{\partial t} = \sum_{n=0}^{\infty} \nu^{-n} \frac{\partial}{\partial t_n}. \tag{4.13}$$

The energy spectrum $\bar{C}^{(2)}$ changes in time at a finite rate since the rate of energy dissipation is finite according to postulate (1.4). The higher-order cumulants, on the other hand, are supposed to change more rapidly since they are subject to larger viscous dissipation than $\bar{C}^{(2)}$. Thus, in accordance with the form of the wavenumber dependence of the cumulants given by (4.11), the cumulants are assumed to depend upon the multiple time scales as follows:

$$\left.\begin{aligned} \bar{C}^{(2)}(t) &= \bar{C}^{(2)}(t_0), \\ \bar{C}^{(3)}(t) &= \bar{C}^{(3)}(t_0, t_1), \\ \bar{C}^{(4)}(t) &= \bar{C}^{(4)}(t_0, t_1, t_2), \quad \text{etc.} \end{aligned}\right\} \tag{4.14}$$

Concerning the order of magnitude of the cumulants, it may be obvious that the energy spectrum $\bar{C}^{(2)}$ is of order $\nu^{\frac{1}{2}}$ since a finite amount of energy is spread over a wavenumber range of order $\nu^{-\frac{1}{2}}$. The magnitude of the higher-order cumulants is supposed to be smaller than $\nu^{\frac{1}{2}}$ since they have an even larger extent than $\bar{C}^{(2)}$. Good support for this estimation is provided by experimental studies referred to in § 1, which show that the velocity correlations of fourth and higher order are related very closely to the second- and third-order ones by the zero-cumulant relations and that the deviation from these relations is confined to a very small region of space and is very small in magnitude. There is no systematic rule for assigning an order of magnitude to each of the higher-order cumulants but their magnitudes are so determined

that they are balanced in the cumulant equations successively. Thus the first three cumulants are expressed as

$$\left.\begin{aligned}\bar{C}^{(2)}(k_1;t_0) &= \nu^{\frac{1}{2}}[\bar{C}_0^{(2)}+\nu\bar{C}_1^{(2)}+\ldots],\\ \bar{C}^{(3)}(k_1,k_2;t_0,t_1) &= \nu^{\frac{3}{2}}[\bar{C}_0^{(3)}+\nu\bar{C}_1^{(3)}+\ldots],\\ \bar{C}^{(4)}(k_1,k_2,k_3;t_0,t_1,t_2) &= \nu^{\frac{5}{2}}[\bar{C}_0^{(4)}+\nu\bar{C}_1^{(4)}+\ldots].\end{aligned}\right\} \tag{4.15}$$

The cumulant equations involve the degenerate cumulants

$$\int \bar{C}^{(n)}\,dh = \bar{\bar{C}}^{(n)}, \quad n \geqslant 3, \tag{4.16}$$

where $\bar{\bar{C}}^{(n)}$ has the same number of independent wavenumber arguments as $\bar{C}^{(n-1)}$. It is natural to assume that $\bar{\bar{C}}^{(n)}$ has the same dependence on the wavenumber and time scales as $\bar{C}^{(n-1)}$ and a magnitude between those of $\bar{C}^{(n)}$ and $\bar{C}^{(n-1)}$. Thus

$$\left.\begin{aligned}\bar{\bar{C}}^{(3)}(k_1;t_0) &= \nu[\bar{\bar{C}}_0^{(3)}+\nu\bar{\bar{C}}_1^{(3)}+\ldots],\\ \bar{\bar{C}}^{(4)}(k_1,k_2;t_0,t_1) &= \nu^2[\bar{\bar{C}}_0^{(4)}+\nu\bar{\bar{C}}_1^{(4)}+\ldots].\end{aligned}\right\} \tag{4.17}$$

On substitution of the expansions (4.13) and (4.15)–(4.17) into (4.8) and (4.9) we obtain the equations governing the coefficient functions of (4.15) and (4.17). To order $\nu^{\frac{1}{2}}$ we have

$$[\partial/\partial t_0 + k_1^2]\,\bar{C}_0^{(2)}(k_1;t_0) = k_1\int \bar{C}_0^{(3)}(k_1,k_2;t_0,t_1)\,dh, \tag{4.18}$$

$$[\partial/\partial t_1 + k_2^2]\,\bar{C}_0^{(3)}(k_1,k_2;t_0,t_1) = k_1\bar{C}_0^{(2)}(k_1;t_0)\,\bar{C}_0^{(2)}(k_1;t_0). \tag{4.19}$$

It should be noted that the fourth-order cumulant $\bar{C}^{(4)}$, being a higher-order term, does not appear in (4.19), so that the multiple-scale expansion acts as a closure assumption in this context.

Since the right-hand side of (4.19) is independent of t_1, it may be integrated at once to give

$$\begin{aligned}\bar{C}_0^{(3)} &= k_2^{-2}[1-\exp(-k_2^2 t_1)]\,k_1\bar{C}_0^{(2)}(k_1;t_0)\,\bar{C}_0^{(2)}(k_1;t_0)\\ &= k_2^{-2}\,[1-\exp(-k_1^2 t_0)]\,k_1\bar{C}_0^{(2)}(k_1;t_0)\,\bar{C}_0^{(2)}(k_1;t_0),\end{aligned} \tag{4.20}$$

where the initial condition

$$C_{ijk}^{(3)}(k,k',k'';0) = 0 \tag{4.21}$$

has been assumed.

Now the pair of equations (4.18) and (4.20) gives, on elimination of $\bar{C}_0^{(3)}$, a closed dynamical equation for $\bar{C}_0^{(2)}$. If we rewrite the symbolic equations (4.18) and (4.20) in terms of the original arguments and restore their tensorial details according to (3.7) and (3.8), we obtain the following equations for the energy spectrum $\phi(k,t)$:

$$[\partial/\partial t + 2\nu k^2]\,\phi(k,t) = \psi(k,t), \tag{4.22}$$

$$\begin{aligned}\psi(k,t) = 4\pi\int_0^\infty dk'\int_{-1}^{1}&\frac{1-\exp[-\nu(k^2+k'^2+k''^2)\,t]}{\nu(k^2+k'^2+k''^2)}\\ &\times[\phi(k',t)-\phi(k,t)]\,\phi(k'',t)\,kk'^3(kk'/k''^2+\mu)\,(1-\mu^2)\,d\mu,\end{aligned} \tag{4.23}$$

where $k''^2 = k^2+k'^2+2\mu kk'$. The initial condition (4.21) for $C_{ijk}^{(3)}$ is written as

$$\psi(k,0) = 0. \tag{4.24}$$

Equations (4.22) and (4.23) constitute the dynamical equations for the energy spectrum based upon the multiple-scale cumulant expansion. The usual energy spectrum function $E(k,t)$ is related to $\phi(k,t)$ through (4.7) and the energy transfer function $T(k,t)$ is expressed similarly as

$$T(k,t) = 4\pi k^2 \psi(k,t). \tag{4.25}$$

5. Numerical calculation

For convenience in numerical work all variables are made non-dimensional with respect to a representative wavenumber k_0 and a representative value of the energy spectrum E_0 as follows:

$$\left.\begin{aligned} &\text{wavenumber,} && \kappa = k/k_0; \\ &\text{time,} && \tau = E_0^{\frac{1}{2}} k_0^{\frac{3}{2}} t; \\ &\text{Reynolds number,} && R = E_0^{\frac{1}{2}}/(\nu k_0^{\frac{1}{2}}); \end{aligned}\right\} \tag{5.1}$$

and the same symbols are used for the non-dimensional forms of ϕ and ψ. Then on elimination of ψ, (4.21) and (4.22) are expressed in non-dimensional form as

$$\left(\frac{\partial}{\partial\tau} + \frac{2}{R}\kappa^2\right)\phi(\kappa,t) = 4\pi R \int_0^\infty d\kappa' \int_{-1}^{1} \frac{1-\exp\left[-(\kappa^2+\kappa'^2+\kappa''^2)\tau/R\right]}{\kappa^2+\kappa'^2+\kappa''^2} \times [\phi(\kappa',\tau)-\phi(\kappa,\tau)]\,\phi(\kappa'',\tau)\,\kappa\kappa'^3(\kappa\kappa'/\kappa''^2+\mu)(1-\mu^2)\,d\mu, \tag{5.2}$$

where $\kappa''^2 = \kappa^2+\kappa'^2+2\mu\kappa\kappa'$.

For the initial condition for (5.2) the following two cases are considered:

$$\text{(I)} \quad \phi(\kappa,0) = (4\pi)^{-1}\exp(-\kappa^2), \tag{5.3}$$

$$\text{(II)} \quad \phi(\kappa,0) = (4\pi)^{-1}\kappa^2\exp(-\kappa^2). \tag{5.4}$$

Cases I and II, which have finite and vanishing energy density at zero wavenumber respectively, represent two typical large-scale structures of turbulence, whose significance will be discussed later. The initial conditions (5.3) and (5.4) may be expressed in terms of the energy spectrum function $E(k,t)$ as

$$\text{(I)} \quad E(k,0) = E_0(k/k_0)^2\exp[-(k/k_0)^2], \tag{5.5}$$

$$\text{(II)} \quad E(k,0) = E_0(k/k_0)^4\exp[-(k/k_0)^2]. \tag{5.6}$$

Likewise, the initial condition (4.23) for ψ is written for the energy transfer function $T(k,t)$ as

$$T(k,0) = 0 \tag{5.7}$$

for both cases.

The integrals on the right-hand side of (5.2) are calculated numerically by using appropriate sum rules at discrete values of κ' and μ and terminating the infinite integral with respect to κ' at a sufficiently large value of κ'. At very large Reynolds numbers the integrand changes rapidly at small κ' and does not vanish even at large κ'. In order to evaluate such an integral accurately and efficiently we employ a non-uniform mesh for κ' whose size is an increasing function of κ'. The following variables are introduced for this purpose:

$$\xi = \log(10\kappa), \quad \eta = 0{\cdot}01R\tau, \quad \tilde{\phi}(\xi,\eta) = 0{\cdot}1\phi(\kappa,\tau). \tag{5.8}$$

In terms of these new variables (5.2) becomes

$$\left(\frac{\partial}{\partial\eta}+\frac{2e^{2\xi}}{R^2}\right)\tilde{\phi}(\xi,\eta) = 3\pi\int_{-\infty}^{\infty} e^{3\xi'}[\tilde{\phi}(\xi',\eta)-\tilde{\phi}(\xi,\eta)]\,d\xi' \times\int_{-1}^{1}\tilde{\phi}(\xi'',\eta)\frac{1-\exp\left[-2e^{\xi+\xi'}(e^{\xi-\xi'}+e^{\xi'-\xi}+\mu)\eta/R^2\right]}{e^{\xi-\xi'}+e^{\xi'-\xi}+\mu} \times\left(\frac{1}{e^{\xi-\xi'}+e^{\xi'-\xi}+2\mu}+\mu\right)(1-\mu^2)\,d\mu. \tag{5.9}$$

The infinite integral with respect to ξ' is terminated at $\xi' = \Xi+\log 2$ ($\kappa' = 0{\cdot}2e^{\Xi}$) and calculated by the trapezoidal rule in the region $-\infty < \xi' \leqslant 0$ ($0 \leqslant \kappa' \leqslant 0{\cdot}1$) and by Simpson's rule in the region $0 < \xi' \leqslant \Xi+\log 2$ ($0{\cdot}1 < \kappa' \leqslant 0{\cdot}2e^{\Xi}$) with a mesh size $\Delta\xi' = \log 1{\cdot}2 = 0{\cdot}18232$. The following values have been chosen for Ξ:

$$\Xi = \begin{cases} 30 & \text{for} \quad R = 5,\ 10,\ 20,\ 100, \\ 40 & \text{for} \quad R = 200,\ 400, \\ 45 & \text{for} \quad R = 800. \end{cases} \tag{5.10}$$

These values of Ξ have been confirmed to be sufficiently large by numerical results. The integration with respect to μ is carried out by Simpson's rule with a mesh size $\Delta\mu = 0{\cdot}1$. The derivative $\partial/\partial\eta$ is replaced by the forward-difference quotient with a mesh size $\Delta\eta = 0{\cdot}0002R$ ($\Delta\tau = 0{\cdot}02$).

In this way (5.9) is solved numerically for the initial conditions (5.3) and (5.4) and the Reynolds numbers listed in (5.10). Thus the energy spectrum function $E(k,t)$ is obtained as a function of the wavenumber k and time t.

Various statistical quantities characterizing turbulence can be derived from numerical results for the energy spectrum, but only representative ones will be presented here.

The kinetic energy of turbulence per unit mass is given by (4.6). This quantity mostly reflects the shape of the energy spectrum $E(k,t)$ in the energy-containing range of the wavenumber.

The skewness of the distribution of the velocity derivative is defined and related to the energy spectrum and the energy transfer function as follows:

$$S(t) = -\frac{\langle(\partial u_1/\partial x_1)^3\rangle}{\langle(\partial u_1/\partial x_1)^2\rangle^{\frac{3}{2}}} = \frac{3\sqrt{30}}{14}\frac{\int_0^\infty k^2T(k,t)\,dk}{\left[\int_0^\infty k^2E(k,t)\,dk\right]^{\frac{3}{2}}}, \tag{5.11}$$

where u_1 is the velocity component along the co-ordinate axis x_1. In contrast to the energy $\mathscr{E}(t)$, the skewness $S(t)$ is mainly determined by the forms of $E(k,t)$ and $T(k,t)$ in the higher wavenumber range, so that it reflects the shape of the energy spectrum $E(k,t)$ beyond the energy-containing range of the wavenumbers.

Lastly, the microscale of the turbulence λ is defined and expressed in terms of the energy spectrum as

$$\lambda(t)^2 = \frac{\langle u_1^2\rangle}{\langle(\partial u_1/\partial x_1)^2\rangle} = \frac{5\int_0^\infty E(k,t)\,dk}{\int_0^\infty k^2E(k,t)\,dk}. \tag{5.12}$$

Sometimes, especially for convenience in comparison with experimental results, non-dimensional variables are defined in terms of $\lambda(t)$ and the root-mean-square velocity $u(t)$, where

$$u(t)^2 = \langle u_1^2 \rangle = \tfrac{1}{3}\langle |\mathbf{u}|^2 \rangle = \frac{2}{3}\int_0^\infty E(k,t)\,dk. \tag{5.13}$$

The relevant Reynolds number is defined as

$$R_\lambda(t) = \frac{u(t)\lambda(t)}{\nu} = \frac{1}{\nu}\frac{10}{3}\frac{\int_0^\infty E(k,t)\,dk}{\left[\int_0^\infty k^2 E(k,t)\,dk\right]^{\frac{1}{2}}}. \tag{5.14}$$

Incidentally it is interesting to note that the initial values of the new Reynolds number $R_\lambda(0)$ corresponding to initial conditions (5.3) and (5.4) are related to the former Reynolds number R as follows:

$$\left.\begin{aligned} &\text{(I)} \quad R = 1{\cdot}0077 R_\lambda(0), \\ &\text{(II)} \quad R = 1{\cdot}0623 R_\lambda(0). \end{aligned}\right\} \tag{5.15}$$

Thus the two Reynolds numbers R and $R_\lambda(0)$ are nearly identical in either case.

6. Energy spectrum

Of all the numerical data concerning the evolution of the energy spectrum function $E(k,t)$ and the energy transfer function $T(k,t)$ those for $R = 20$ and 800 are chosen as representative data and shown graphically in figures 1(*a*)–(*d*).† For all Reynolds numbers examined the energy spectrum $E(k,t)$ is found to be positive definite at all times.

It is not evident in figures for $R = 20$ but may clearly be seen from figures for large Reynolds numbers such as $R = 800$ that there is an abrupt change in the behaviour of $E(k,t)$ and $T(k,t)$ in time at about $t = 4$ for case I and at about $t = 3$ for case II. In the period preceding this change both functions undergo rapid deformation from their initial forms into similar forms, which are nearly identical for cases I and II but apparently depend upon R. In the later period, on the other hand, they change slowly and similarly in time. The presence of these two periods may also be observed in other statistical variables which will be described later on, and therefore this seems to be a characteristic feature of the evolution of decaying turbulence at large Reynolds numbers. For later convenience the above two periods are referred to as the initial and similarity periods respectively.‡

The form of the spectrum $E(k,t)$, especially its structure at higher wavenumbers, is displayed more clearly on a logarithmic scale as shown in figures 2(*a*)–(*d*). The distinction between the initial and similarity periods is more evident in these figures.

There are some remarkable features in the evolution of the spectrum shown in the above figures. First, the positive slopes of $E(k,t)$ at very low wavenumbers, which are

† Statistical functions including $E(k,t)$ and $T(k,t)$ have been calculated for all combinations of cases I and II and $R = 5$, 10, 20, 100, 200, 400, 800. The figures which are not displayed in this paper are available on request from the first author (T. T.).

‡ In common usage the initial period of decay includes both the initial and the similarity period defined above.

2 and 4 for cases I and II respectively according to (5.5) and (5.6), are almost invariant in time. Thus the spectrum in the very low wavenumber range is entirely fixed by the initial condition, reflecting the well-known permanence of the large-scale components of turbulence. Second, in the similarity period, the higher wavenumber part of the spectrum is not influenced appreciably by the difference between cases I and II at very low wavenumbers but has a nearly identical form for both cases. The existence of such a universality in the spectrum in the higher wavenumber range clearly suggests the possibility of constructing a theory of a universal spectrum for decaying turbulence using the present results. Such a theory will be dealt with in §§ 7 and 8.

The more detailed structure of the spectrum in the similarity period is dependent upon the Reynolds number, so that it will be described below for small and large Reynolds numbers in turn.

At small Reynolds numbers such as $R = 20$ the spectrum preserves its exponential form throughout its variation in time. A closer inspection of the spectrum reveals that its dependence on the wavenumber is not precisely that of $\exp(-2\nu k^2 t)$ as would be expected from the linearized form of (5.2) and the initial conditions (5.5) and (5.6) but is more closely represented by

$$E(k,t) \simeq \exp(\sigma k^{1.5}) \tag{6.1}$$

as $k \to \infty$, where σ is a constant dependent upon ν and t. This result shows that even at small Reynolds numbers the spectrum does not tend to the purely viscous spectrum as the wavenumber increases indefinitely. This problem will be discussed later, in § 8.1.

At large Reynolds numbers such as $R = 200$–800 the spectrum in the universal wavenumber range is composed of three parts having different functional forms.

(i) In the lowest subrange of the universal wavenumber range, the spectrum is expressed as

$$E(k,t) \propto k^{-\frac{5}{3}}, \tag{6.2}$$

which has exactly the same power as Kolmogorov's (1941 *a*) inertial-subrange spectrum. The part of the subrange in which (6.2) is valid increases indefinitely with Reynolds number. This result is in accordance with Kolmogorov's second hypothesis, which assumes the existence of the inertial subrange at very large Reynolds numbers.

The $-\frac{5}{3}$ power spectrum has been observed by many experimentalists in various turbulent flows with extremely large Reynolds numbers either in nature or in the laboratory. Grant, Stewart & Moilliet (1962) and Grant & Moilliet (1962) found this spectrum in tidal streams, Wyngaard & Pao (1972) found it in atmospheric winds, Gibson (1962, 1963) found it in a jet and Gibson & Schwarz (1963), Kistler & Vrebalovich (1961, 1966) and Schedvin, Stegen & Gibson (1974) found it in grid-generated turbulence. Also, many other measurements are referred to in the monograph by Monin & Yaglom (1975). The present result will be compared with these measurements in § 9.2.

(ii) Next to the previous subrange, there exists a subrange in which the spectrum may be expressed as

$$E(k,t) \propto k^{-1}. \tag{6.3}$$

As the Reynolds number increases, this subrange is shifted to higher wavenumbers without changing its width on a logarithmic scale but becomes wider on a linear scale.

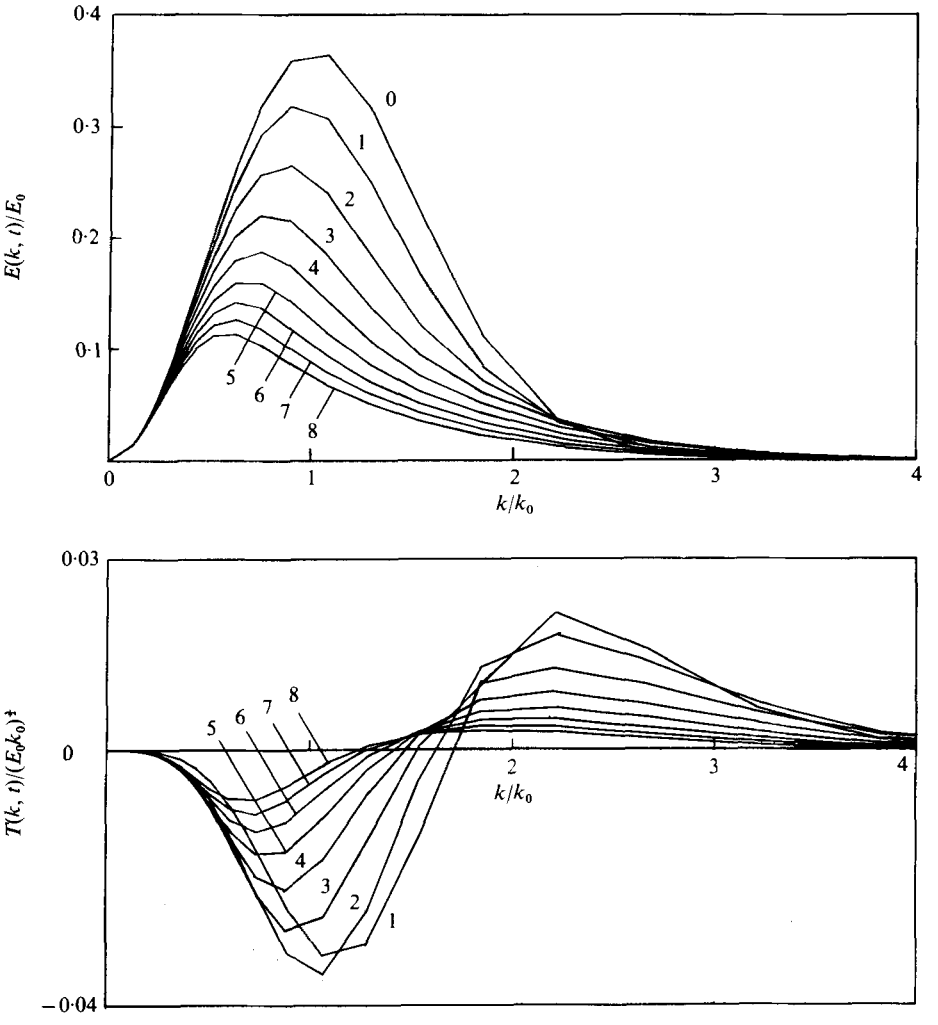

FIGURE 1 (*a*). For legend see p. 115.

It may be interesting to note that the spectrum (6.3) is identical to that of turbulence which is composed of a random collection of extremely fine vortex filaments of any shape. It is a matter of elementary calculus to show that, irrespective of the spatial dimension, the spectrum functions $E(k,t)$ for random collections of line vortices and plane vortices are proportional to k^{-1} and k^{-2} respectively. Thus the existence of the spectrum (6.3) indicates that the smallest structure of turbulence at large Reynolds numbers consists mostly of line vortices.

So far no experimental evidence has been obtained for the existence of the k^{-1} subrange adjacent to the $k^{-\frac{5}{3}}$ subrange. It should be noted, however, that experimental results are mostly presented in the form of the one-dimensional spectrum, $F(k,t)$ say, which is related to the three-dimensional spectrum $E(k,t)$ by

$$F(k,t) = \frac{1}{2}\int_k^\infty \left(1-\frac{k^2}{k'^2}\right)\frac{1}{k'}E(k',t)\,dk'. \tag{6.4}$$

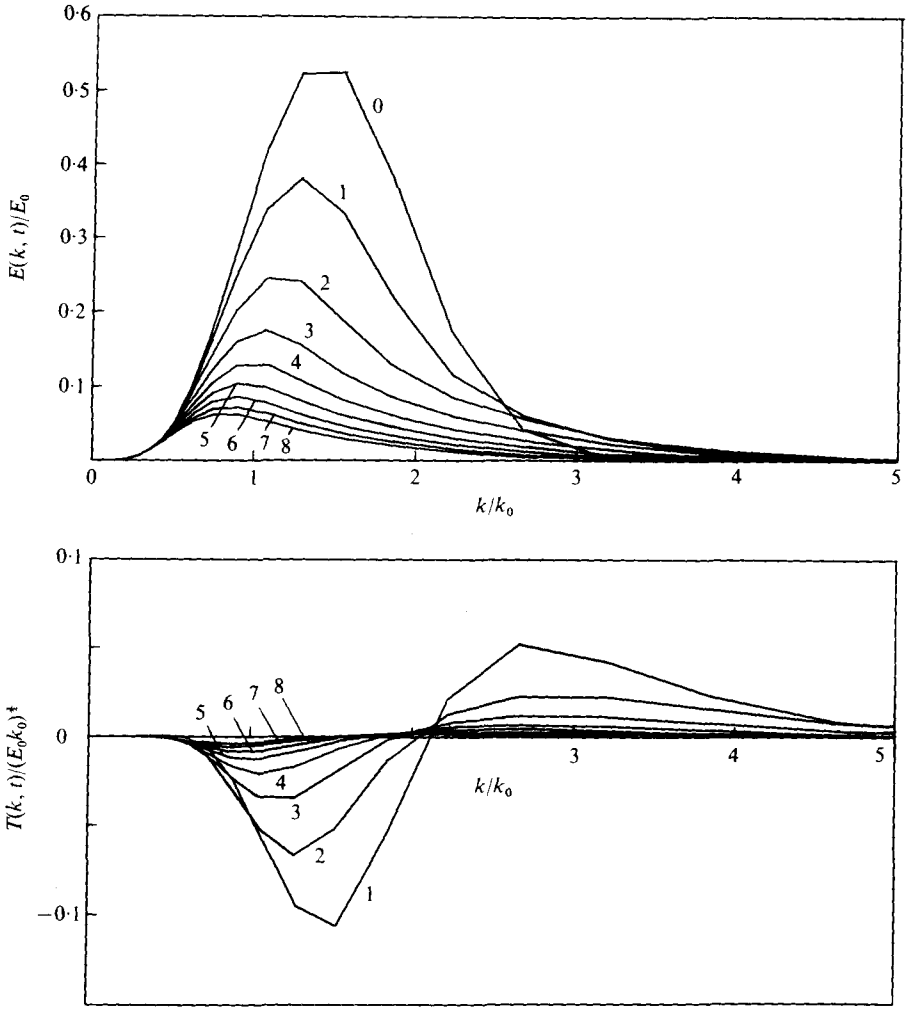

FIGURE 1 (*b*). For legend see p. 115.

The k^{-1} subrange in $E(k,t)$ is smoothed out through this transformation and there remains only a slightly more gentle slope next to the $k^{-\frac{5}{3}}$ subrange in $F(k,t)$. Thus it is rather difficult to tell whether the k^{-1} subrange in the three-dimensional spectrum is compatible with the measured one-dimensional spectra or not, and a more precise comparison of theoretical and experimental spectra seems to be needed before a definite conclusion can be obtained.

Incidentally, it may be interesting to note that a combined $k^{-\frac{5}{3}}$ and k^{-1} spectrum was proposed by Batchelor (1959) for the spectrum of temperature fluctuations in turbulence at large Prandtl numbers and confirmed experimentally by the measurements of Grant *et al.* (1968).

(iii) At still higher wavenumbers, the spectrum $E(k,t)$ takes the exponential form (6.1). Thus, according to the present theory, the asymptotic form of the spectrum for very high wavenumbers is given by (6.1) irrespective of the Reynolds number.

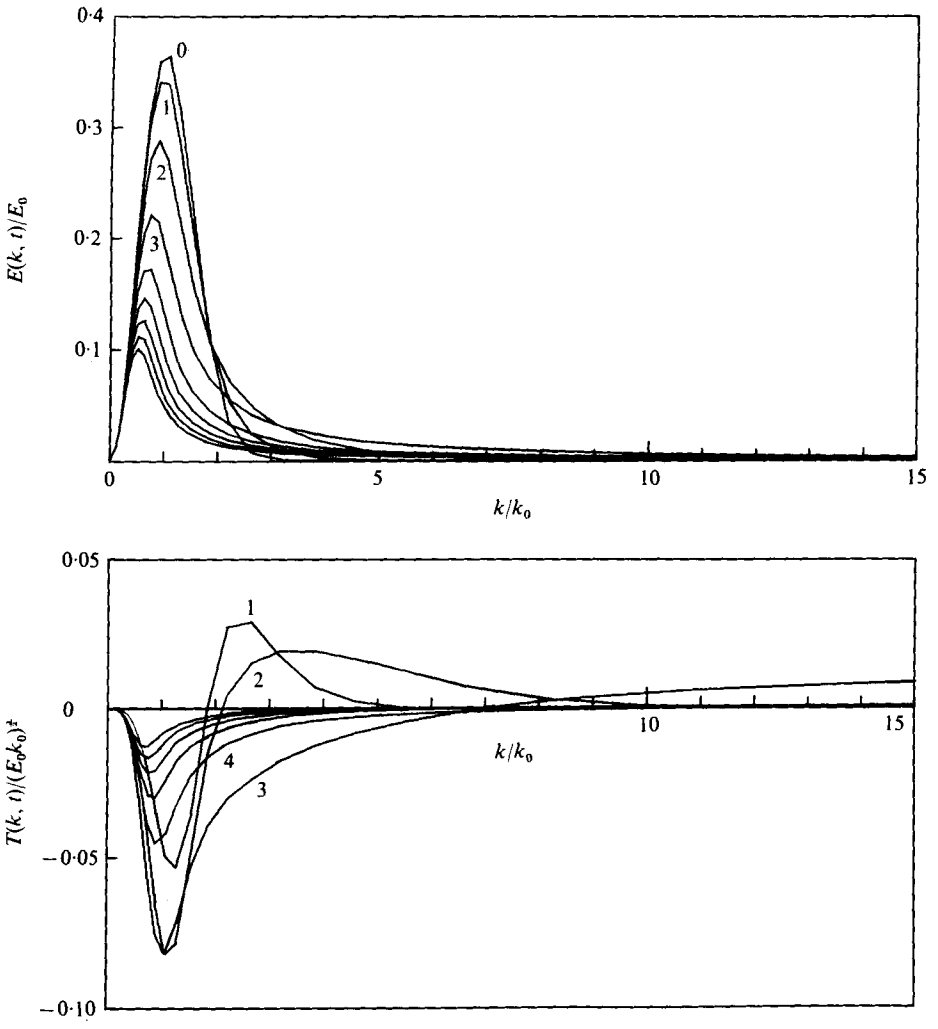

FIGURE 1 (*c*). For legend see facing page.

It is rather difficult to deduce a definite asymptotic form from measured spectra, which generally show erratic behaviour due to increasing noise at high wavenumbers. A theoretical form of the spectrum at very high wavenumbers was proposed by Pao (1965, 1968). Assuming that the rate of energy transfer across a wavenumber k is dependent on the energy dissipation ϵ and the wavenumber k, he obtained the following spectrum through dimensional reasoning:

$$E(k) = K\epsilon^{\frac{2}{3}}k^{-\frac{5}{3}}\exp\left[-\tfrac{3}{2}K\nu\epsilon^{-\frac{1}{3}}k^{\frac{4}{3}}\right] \tag{6.5}$$

for $k \gg k_0$, where K is Kolmogorov's constant and is defined in (8.11) below. It is interesting to note that the wavenumber dependence $k^{\frac{4}{3}}$ of the exponential factor is fairly close to the $k^{1\cdot5}$ of (6.1). Pao compared the theoretical form (6.5) with experimental spectra with various values for K. General agreement was attained with $K = 1\cdot7$ but the comparison is not conclusive owing to the scatter in the experimental data.

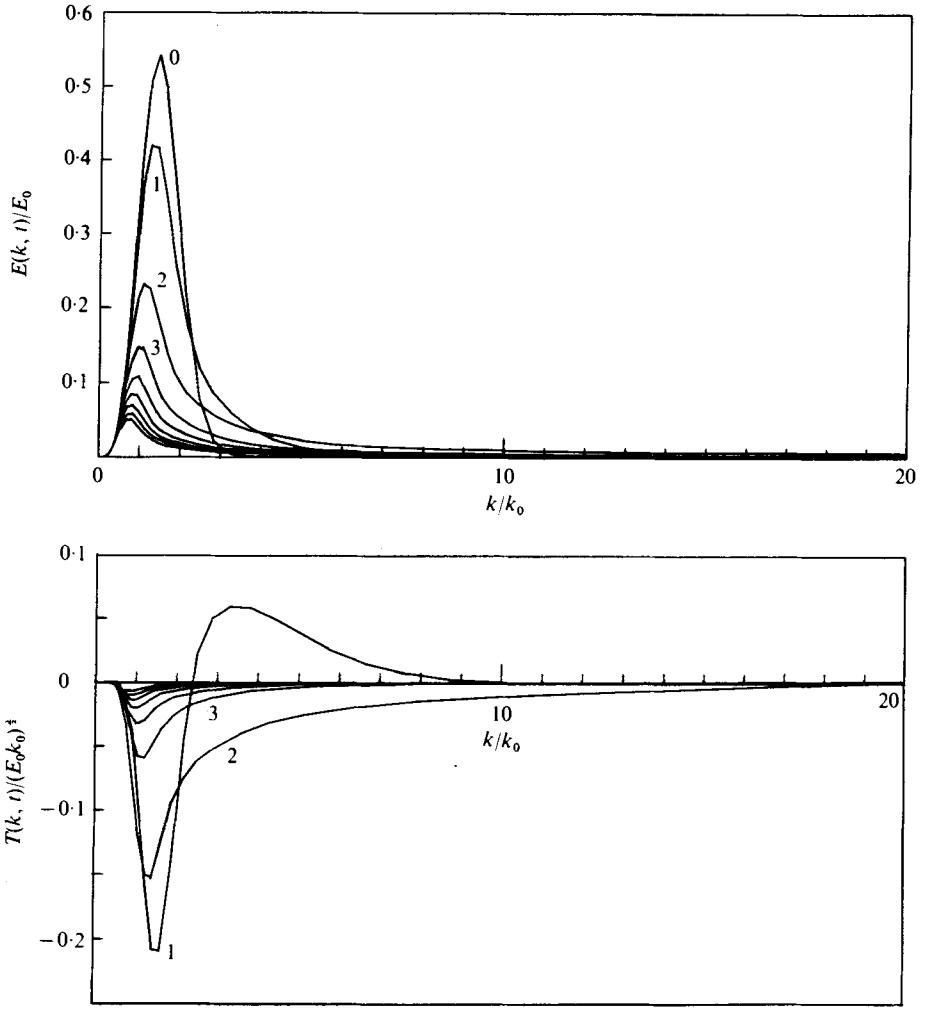

FIGURE 1. The energy spectrum function $E(k, t)$ and the energy transfer function $T(k, t)$. In all the figures in this paper the numbers by the curves denote the non-dimensional time $\tau = E_0^{\frac{1}{2}}k_0^{\frac{3}{2}}t$. (*a*) Case I, $R = 20$. (*b*) Case II, $R = 20$. (*c*) Case I, $R = 800$. (*d*) Case II, $R = 800$.

7. Similarity laws for energy spectrum

If the energy spectrum function $E(k, t)$ satisfies a similarity law with respect to Reynolds number and time within a certain wavenumber range, it must be expressed in the following non-dimensional form in this wavenumber range:

$$E(k,t)/E_0 = R^{-\alpha}\tau^{-\beta}F(\kappa/(R^{\gamma}\tau^{\delta})), \tag{7.1}$$

where the exponents α, β, γ and δ are constants and F is a non-dimensional function.

The similarity is confirmed geometrically by making the spectral curves in the logarithmic representation coincide with each other over a wavenumber range through suitable parallel displacements. In practice, the best coincidence is attained by minimizing the mean-square distance between the curves. Then the values of the

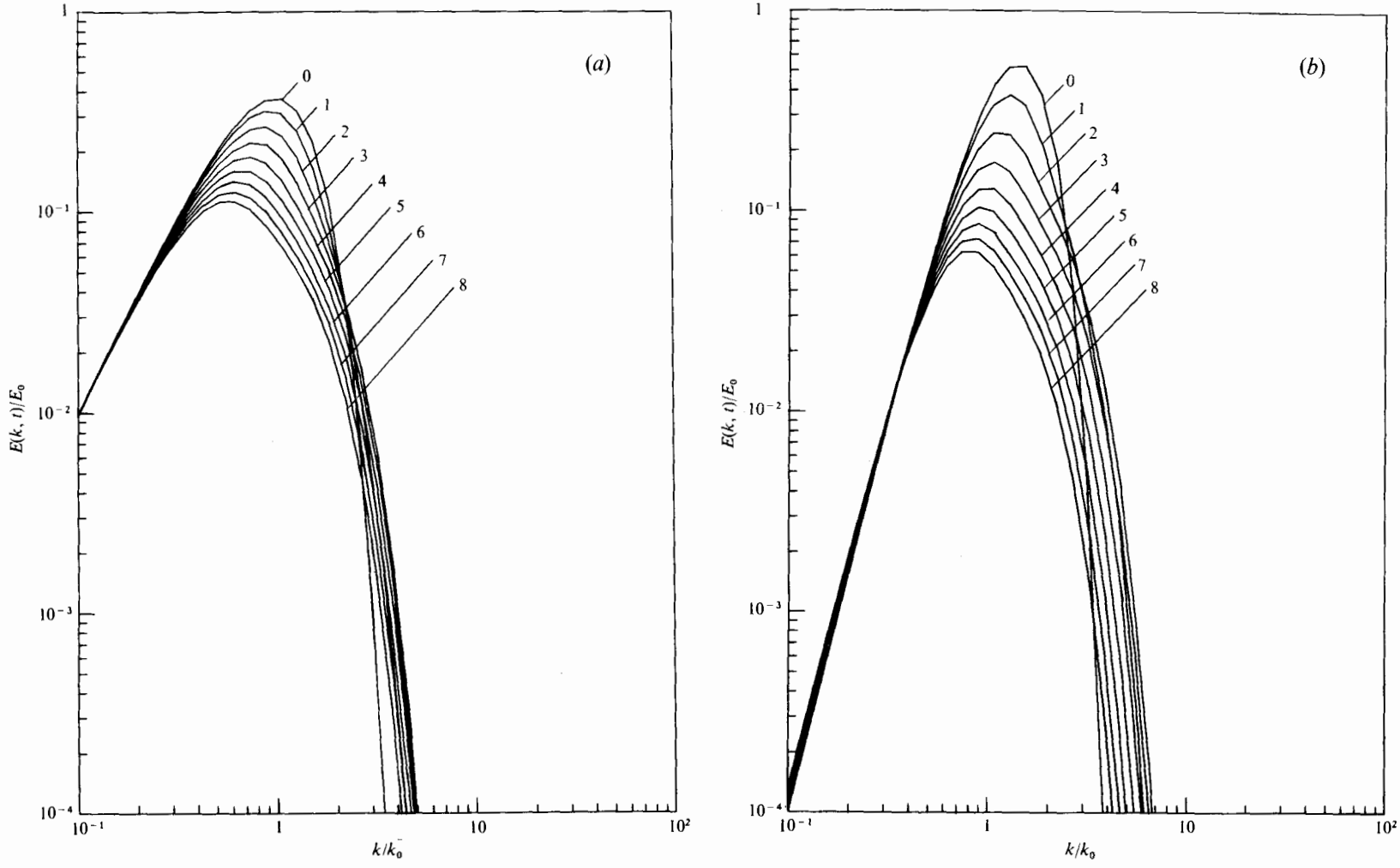

FIGURES 2 (*a*, *b*). For legend see facing page.

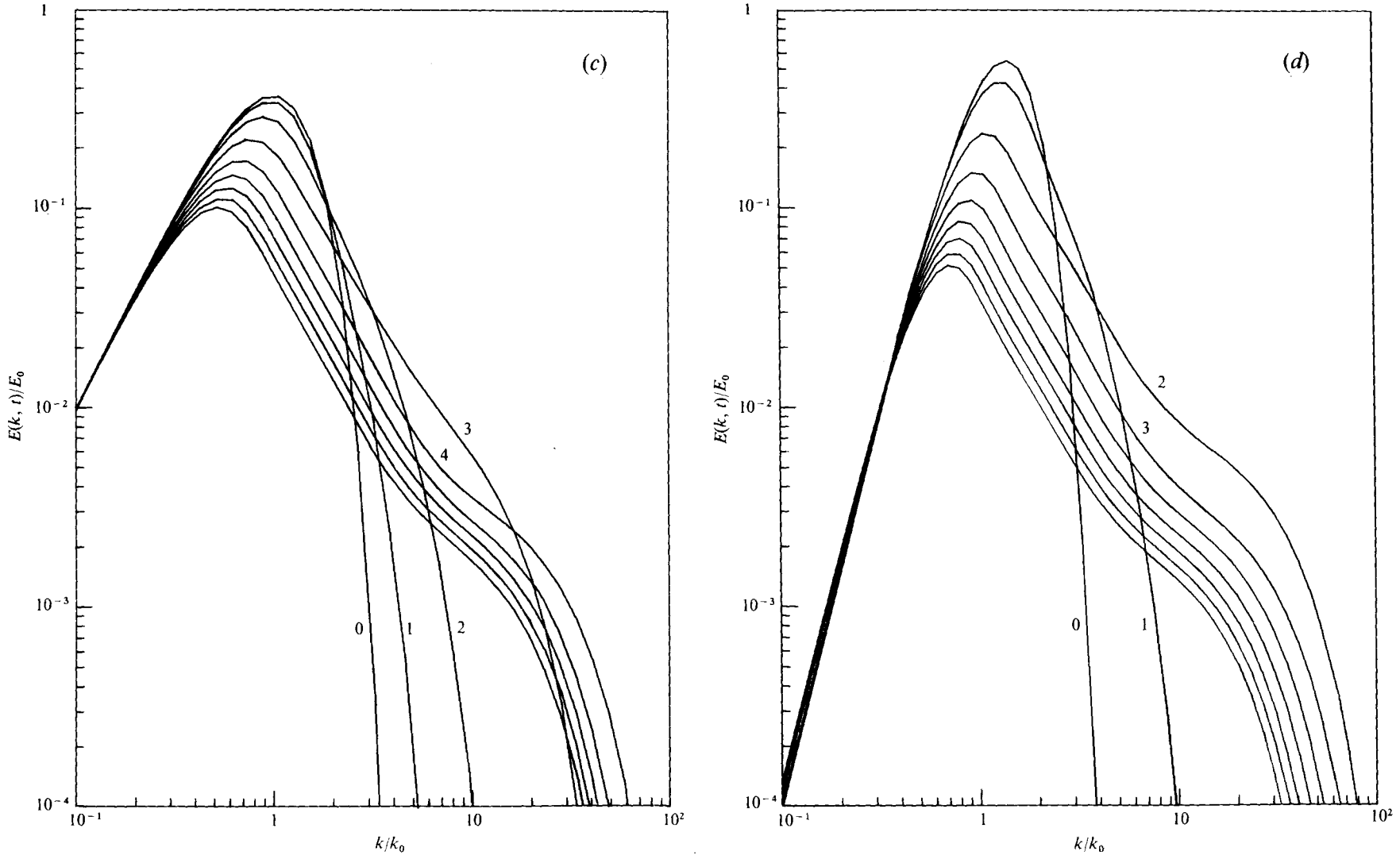

FIGURE 2. The energy spectrum function $E(k, t)$ on a logarithmic scale. (*a*) Case I, $R = 20$. (*b*) Case II, $R = 20$. (*c*) Case I, $R = 800$. (*d*) Case II, $R = 800$.

exponents α and γ are obtained from the sizes of the vertical and horizontal displacements respectively of the curves for different Reynolds numbers, while the values of β and δ are determined from the corresponding displacements of the curves for different times. The function F is obtained from the mean of the superimposed curves.

As mentioned before, there is no single similarity law which is valid at all wavenumbers, but there do exist two different similarity laws satisfied in the energy-containing and the universal ranges separately.

7.1. *Energy-containing range*

First, the curves for a fixed Reynolds number and different times ($\tau = 0, 1, 2, \ldots, 8$) are brought into coincidence with each other over the wavenumber range $0{\cdot}2 \leqslant \kappa \leqslant 2{\cdot}0$, which roughly corresponds to the energy-containing range. The results for $R = 800$ are shown in figures 3(*a*) and (*b*) for cases I and II respectively; here the curves for $\tau = 8$ have been fixed as reference curves. The coincidence appears to be perfect for the curves belonging to the similarity period, i.e. $\tau \geqslant 4$ for case I and $\tau \geqslant 3$ for case II. Next, the resulting curves for different Reynolds numbers ($R = 200$, 400 and 800) are made to coincide with each other over the same wavenumber range. The numerical values of the exponents thus obtained for the energy-containing range, which are denoted by the suffix 1, are listed in table 1. Errors in the numerical values are found to be at most a few per cent. The most remarkable of the above results is that $\alpha_1 \fallingdotseq 0$ and $\gamma_1 \fallingdotseq 0$ or, in other words, that the structure of the large-scale components of turbulence, which contain essentially all the turbulent energy, is independent of the Reynolds number so long as it is very large. The shape of the mean curve in the energy-containing range, or the function $F = F_1$, say, is different for cases I and II, reflecting the difference in the initial spectra at very low wavenumbers, but its shape beyond the maximum is almost identical for the two cases.

Once the similarity of the energy-containing spectrum with respect to time has been established, the law of decay of the turbulent energy may be derived immediately. Substitution from (7.1), with the suffix 1, into (4.6) gives

$$\begin{aligned} \mathscr{E}(t) &= E_0 k_0 R^{-\alpha_1} \tau^{-\beta_1} \int_0^\infty F_1(\kappa/(R^{\gamma_1}\tau^{\delta_1}))\, d\kappa \\ &= E_0 k_0 R^{-\alpha_1+\gamma_1} \tau^{-\beta_1+\delta_1} \int_0^\infty F_1(s)\, ds. \end{aligned} \tag{7.2}$$

By making use of the numerical values in table 1, we obtain the following laws for the decay of energy:

$$\text{(I)} \quad \mathscr{E}(t) \propto R^{0{\cdot}01} \tau^{-1{\cdot}20}, \tag{7.3}$$

$$\text{(II)} \quad \mathscr{E}(t) \propto R^{0{\cdot}01} \tau^{-1{\cdot}39}. \tag{7.4}$$

Obviously the energy $\mathscr{E}(t)$ does not depend appreciably on the Reynolds number R for either case.

It is an immediate consequence of (7.3) and (7.4) that the energy dissipation rate

$$\epsilon(t) = -\frac{d}{dt}\mathscr{E}(t) = -\frac{d}{dt}\int_0^\infty E(k,t)\, dk \tag{7.5}$$

is independent of the Reynolds number, and thus the viscosity ν. This conclusion is in accordance with postulate (1.4) or (1.5) and thus proves the self-consistency of the present scheme of approximation.

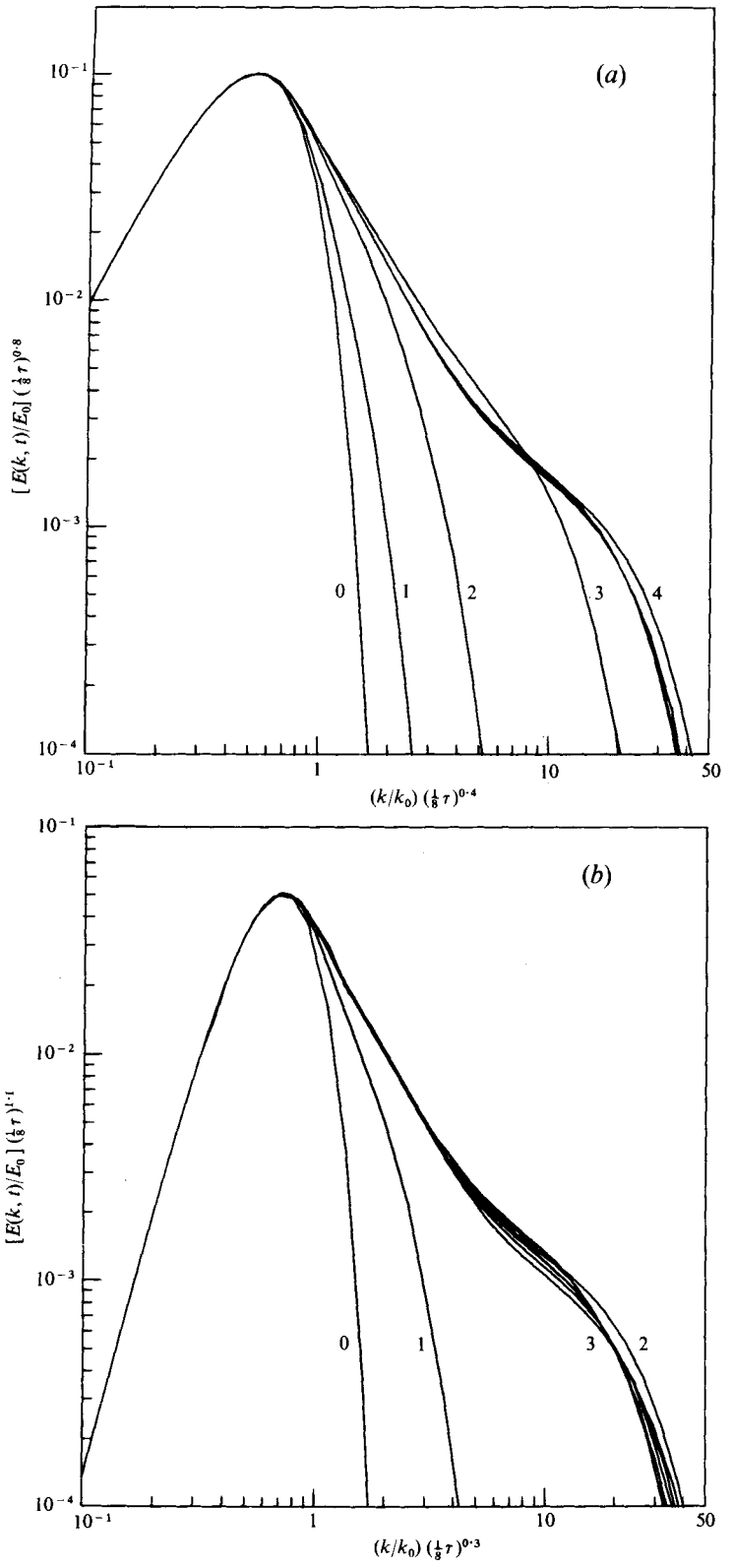

FIGURE 3. The inviscid similarity of the energy spectrum function $E(k, t)$ for $R = 800$. (*a*) Case I. (*b*) Case II.

	Case I		Case II	
	Numerical	Analytical	Numerical	Analytical
α_1	0·00	0·0	0·00	0·0
β_1	0·80	$\frac{4}{5} = 0{\cdot}8$	1·09	$\frac{8}{7} = 1{\cdot}14$
γ_1	0·01	0·0	0·01	0·0
δ_1	−0·40	$-\frac{2}{5} = -0{\cdot}4$	−0·30	$-\frac{2}{7} = -0{\cdot}29$

TABLE 1. Similarity exponents for the energy-containing range.

7.2. *Universal range*

The similarity of the spectrum in the universal range is determined by the same method, i.e. by requiring coincidence of the curves in the wavenumber range $3{\cdot}0 \leqslant \kappa \leqslant 30$, which is roughly the common part of the universal range for the Reynolds numbers examined. The results are shown in figures 4(*a*) and (*b*) for cases I and II respectively; here the curves for $R = 800$ and $\tau = 8$ have been fixed as the reference curves. The coincidence of the curves is very good, and unlike that for the energy-containing range, the shape of the mean curve for the universal range, or the function $F = F_2$, say, is nearly identical for cases I and II.

The numerical values of the exponents for the universal range, which are denoted by the suffix 2, are listed in table 2, where again errors are within a few per cent. It may be noted that the values of α_2 and γ_2, representing the dependence upon Reynolds number, are the same for cases I and II, whereas those of β_2 and δ_2, representing the time dependence, are slightly different for the two cases, possibly owing to the different rates of energy supply from the energy-containing range.

Now that numerical values of the exponents for the universal range have been determined, the similarity form of the energy spectrum $E(k, t)$ in each subrange of the universal range can be derived from the general formula (7.1).

(i) $-\frac{5}{3}$ *power subrange.* Assuming the function F_2 in (7.1) to be of the form (6.2) and substituting the numerical values of the exponents from table 2, we obtain the following similarity forms of the spectrum in the $-\frac{5}{3}$ power subrange:

$$\text{(I)} \quad E(k,t)/E_0 = 1{\cdot}2R^{-0{\cdot}04}\tau^{-1{\cdot}44}\kappa^{-\frac{5}{3}}, \tag{7.6}$$

$$\text{(II)} \quad E(k,t)/E_0 = 1{\cdot}0R^{-0{\cdot}02}\tau^{-1{\cdot}57}\kappa^{-\frac{5}{3}}, \tag{7.7}$$

where the coefficients have been determined from the mean curves in figures 4(*a*) and (*b*). It is obvious from the above result that in this subrange the spectrum $E(k, t)$ is independent of the Reynolds number R, and thus the viscosity ν. So Kolmogorov's second hypothesis, which assumes independence of the spectrum from the viscosity, is actually satisfied here, so that the spectra (7.6) and (7.7) are nothing but Kolmogorov's *inertial-subrange* spectrum.

(ii) -1 *power subrange.* The similarity form of the spectrum in the -1 power subrange is obtained in the same way as that in (i) as follows:

$$\text{(I)} \quad E(k,t)/E_0 = 4{\cdot}8R^{-0{\cdot}51}\tau^{-1{\cdot}09}\kappa^{-1}, \tag{7.8}$$

$$\text{(II)} \quad E(k,t)/E_0 = 4{\cdot}0R^{-0{\cdot}50}\tau^{-1{\cdot}18}\kappa^{-1}. \tag{7.9}$$

These spectra are dependent on both the Reynolds number and time.

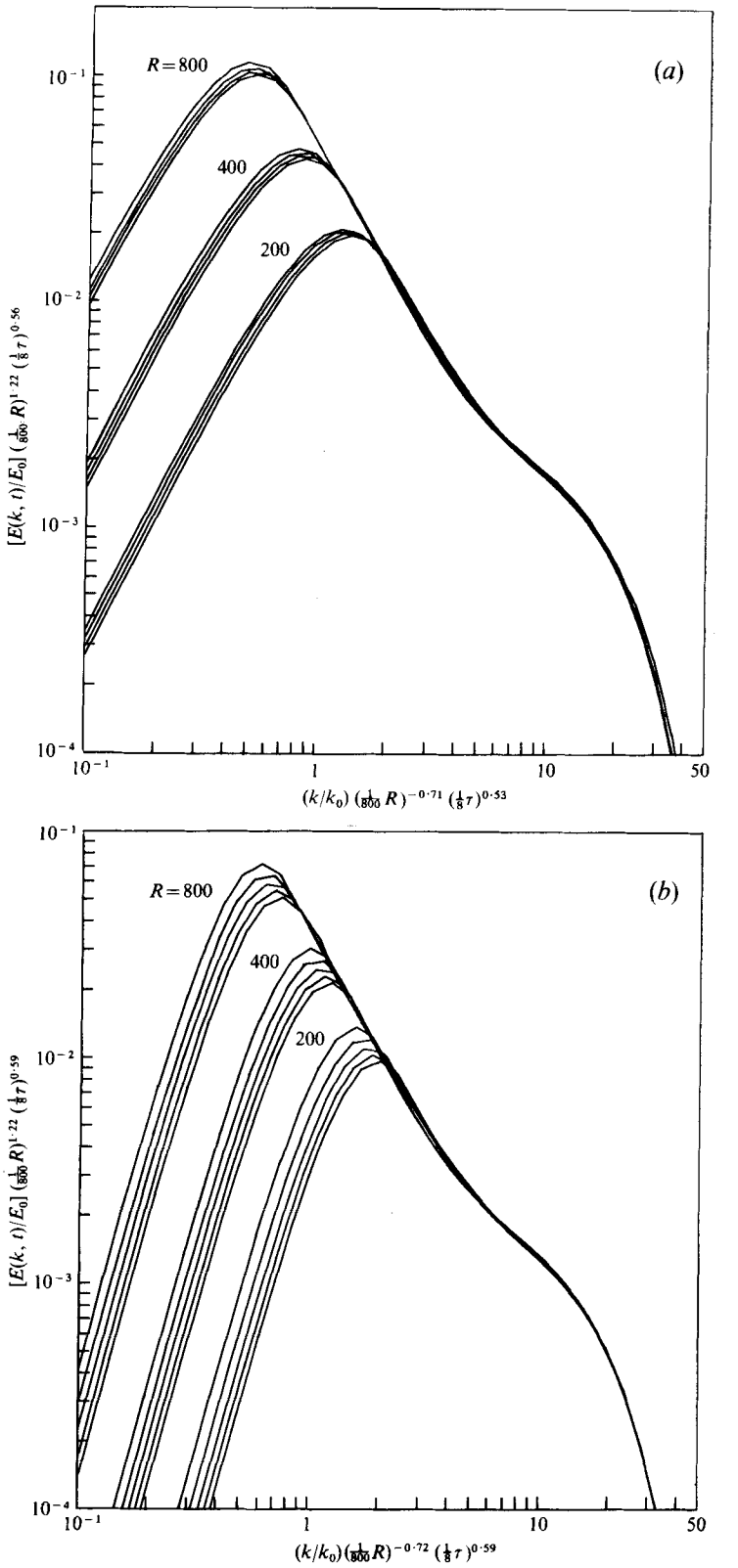

FIGURE 4. The universal similarity of the energy spectrum function $E(k, t)$. (*a*) Case I. (*b*) Case II.

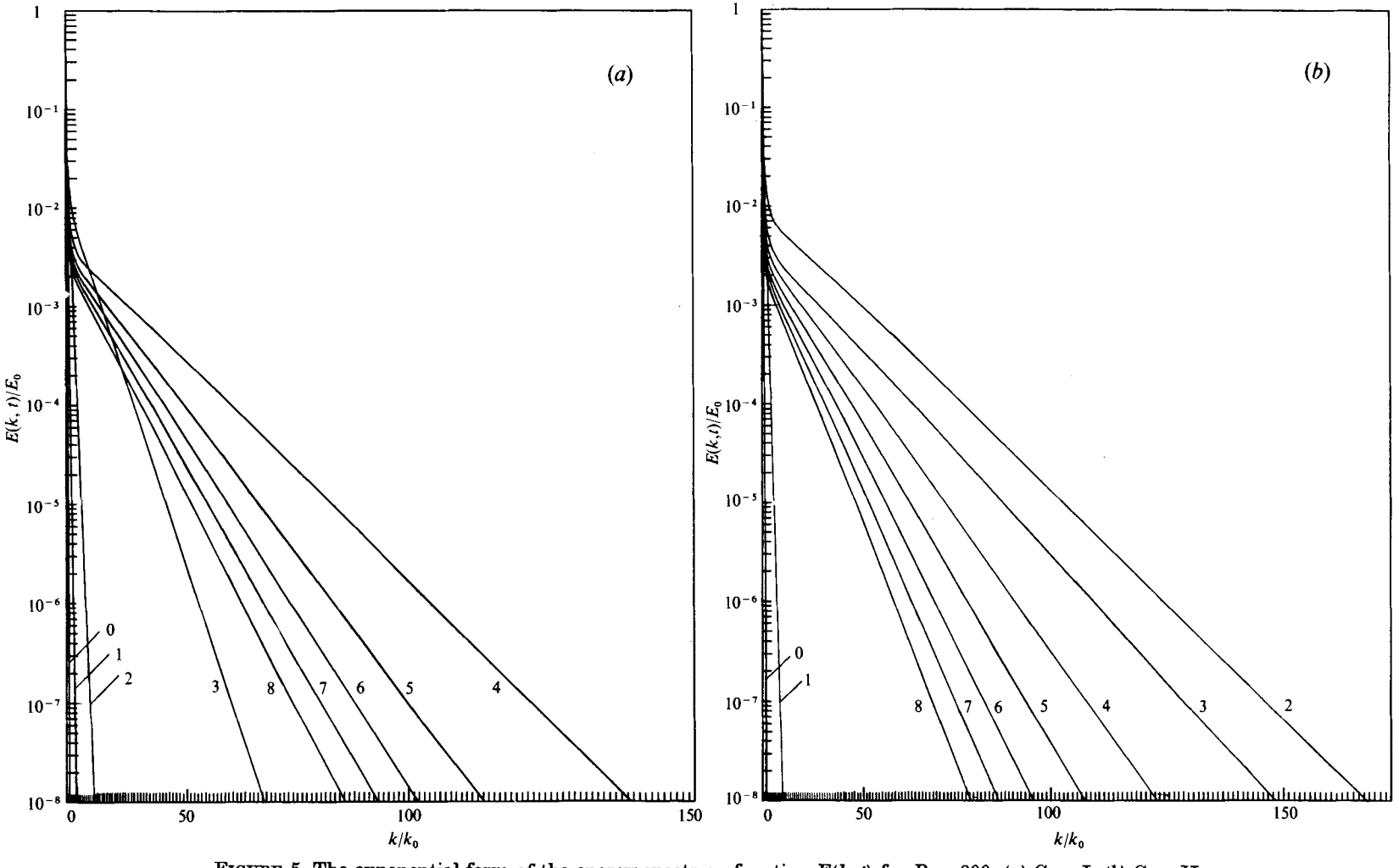

FIGURE 5. The exponential form of the energy spectrum function $E(k, t)$ for $R = 800$. (*a*) Case I. (*b*) Case II.

	Case I		Case II	
	Numerical	Analytical	Numerical	Analytical
α_2	1·22	$\frac{5}{4} = 1{\cdot}25$	1·22	$\frac{5}{4} = 1{\cdot}25$
β_2	0·56	$\frac{11}{20} = 0{\cdot}55$	0·59	$\frac{17}{28} = 0{\cdot}61$
γ_2	0·71	$\frac{3}{4} = 0{\cdot}75$	0·72	$\frac{3}{4} = 0{\cdot}75$
δ_2	−0·53	$-\frac{11}{20} = -0{\cdot}55$	−0·59	$-\frac{17}{28} = -0{\cdot}61$

TABLE 2. Similarity exponents for the universal range.

(iii) *Exponential subrange.* The functional form (6.1) of the spectrum at very high wavenumbers is clearly seen from the plots of $\log E(k,t)$ *vs.* $k^{1\cdot5}$ shown in figures 5(*a*) and (*b*). All curves are straight with good accuracy for κ higher than about 15.

The similarity form of the spectrum in the exponential subrange is obtained in the same way as before and may be expressed as follows:

$$\text{(I)} \quad \log\left(E(k,t)/E_0\right) \simeq -3{\cdot}7R^{-1\cdot07}\tau^{0\cdot80}\kappa^{1\cdot5}, \tag{7.10}$$

$$\text{(II)} \quad \log\left(E(k,t)/E_0\right) \simeq -3{\cdot}6R^{-1\cdot08}\tau^{0\cdot89}\kappa^{1\cdot5} \tag{7.11}$$

for $\kappa \to \infty$.

8. Inviscid similarity and Kolmogorov's similarity

It has been shown in preceding sections that the energy spectrum $E(k,t)$ satisfies different similarity laws with respect to Reynolds number and time in various wavenumber ranges and subranges. The differences between these similarity laws are accounted for in §8.1 by comparing the magnitude of the nonlinear energy transfer with that of the viscous dissipation of energy. Next, it is shown in §8.2 that the law of energy decay can be derived from the inviscid similarity law in the energy-containing range and the inertial subrange combined with Kolmogorov's similarity law in the universal range.

8.1. *Energy transfer and energy dissipation*

The spectrum $E(k,t)$ consists at large Reynolds numbers of several component spectra which have their own similar forms and wavenumber ranges of validity. The characteristics of these component spectra are most clearly exhibited in figures which show the energy spectrum function $E(k,t)$, the energy transfer function $T(k,t)$ and the energy dissipation function

$$D(k,t) = 2\nu k^2 E(k,t) \tag{8.1}$$

together. Some examples of such figures are given in figures 6(*a*)–(*d*), where the arcsin–hyperbolic scale has been adopted in order to give an even appearance to the curves by suppressing larger variations along either axis.

(i) It may be noticed in the figures for large Reynolds numbers that throughout the energy-containing range and the inertial ($-\frac{5}{3}$ power) subrange the energy dissipation is much smaller in magnitude than the energy transfer:

$$D(k,t) \ll |T(k,t)|. \tag{8.2}$$

It is indeed this condition that makes the spectra in the energy-containing range and the inertial subrange essentially independent of the viscosity. As already seen in §7,

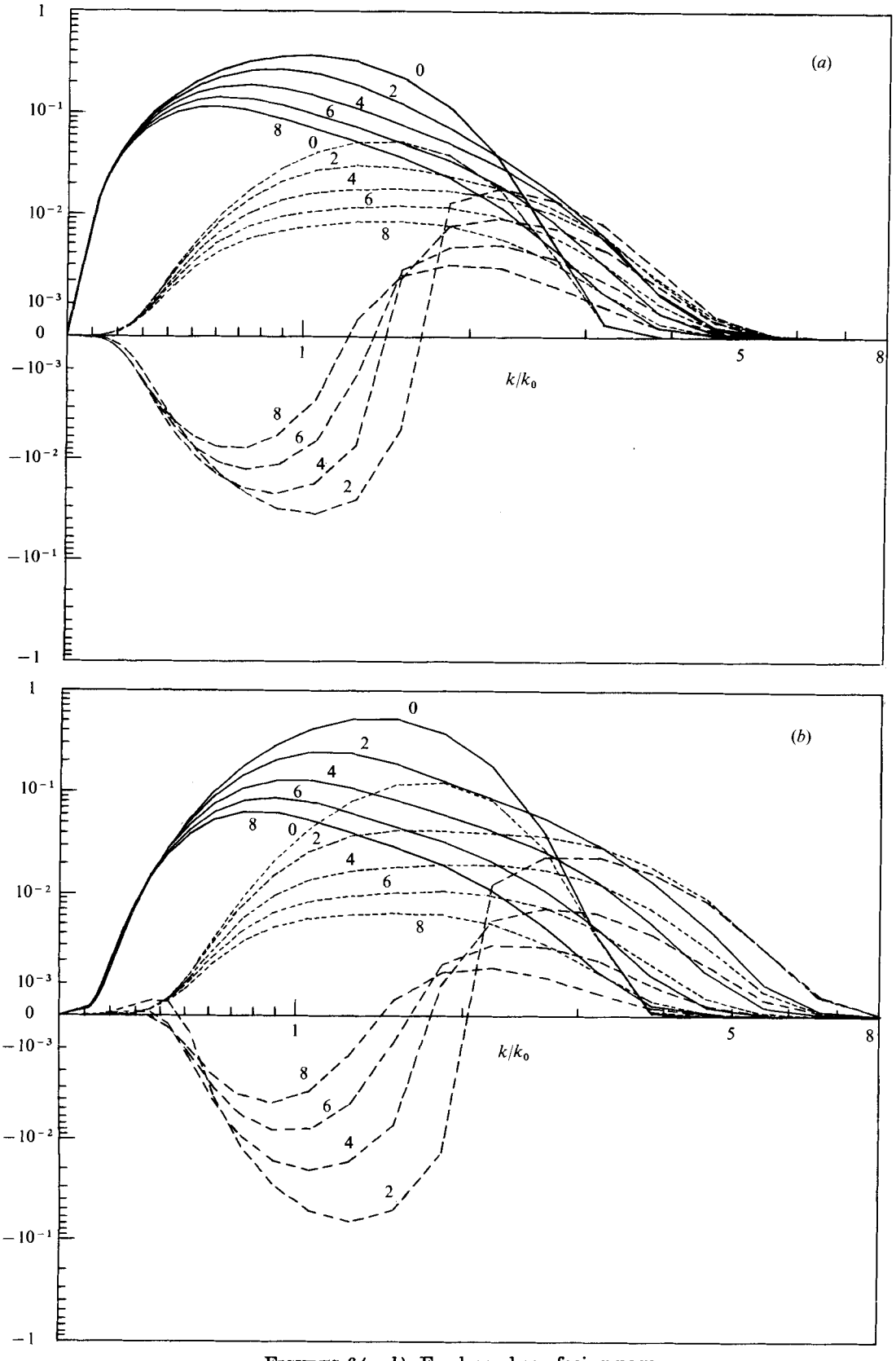

FIGURES 6 (*a*, *b*). For legend see facing page.

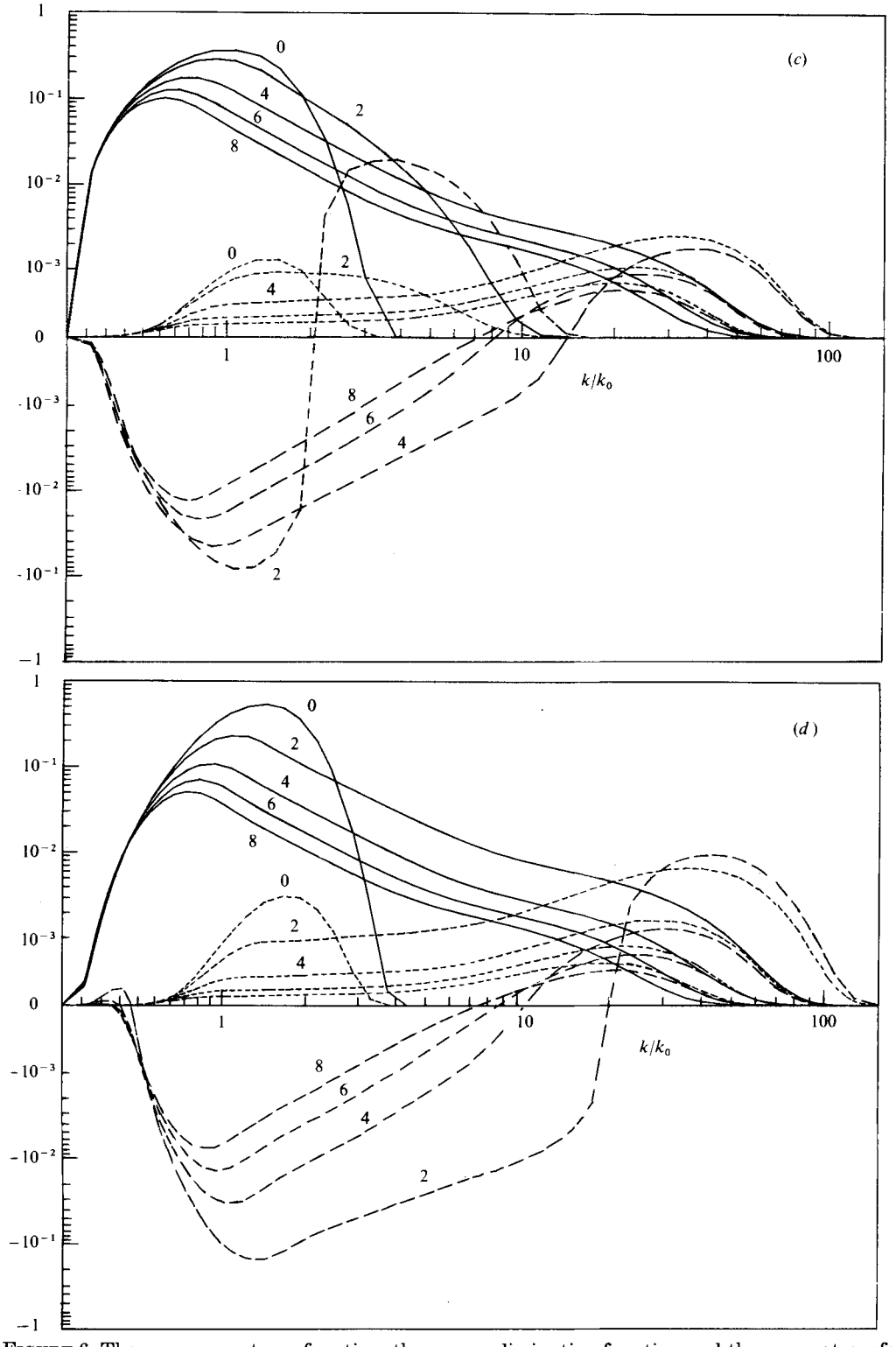

FIGURE 6. The energy spectrum function, the energy dissipation function and the energy transfer function. ——, $E(k, t)/E_0$; – – –, $2\nu k^2 E(k, t)/(E_0 k_0)^{\frac{3}{2}}$; — — —, $T(k, t)/(E_0 k_0)^{\frac{3}{2}}$. All curves are plotted on an arcsin–hyperbolic scale. (*a*) Case I, $R = 20$. (*b*) Case II, $R = 20$. (*c*) Case I, $R = 800$. (*d*) Case II, $R = 800$.

the inviscid similarity in the energy-containing range is consistent with Kolmogorov's first similarity hypothesis while that in the inertial subrange agrees with his second similarity hypothesis. Therefore Kolmogorov's similarity law based upon these two hypotheses is satisfied by the present numerical results for the decaying turbulence. A treatment of the decay process of turbulence using Kolmogorov's similarity law will be made in §8.2.

It should be noted that condition (8.2) is somewhat different from the usual condition for Kolmogorov's inertial-subrange spectrum. This spectrum was originally derived for locally isotropic turbulence, in which the universal-range spectrum is assumed to be stationary, i.e. $\partial E(k,t)/\partial t \simeq 0$. Then the inertial subrange exists under the condition that both $D(k,t)$ and $T(k,t)$ are nearly zero. In the present case, on the other hand, $T(k,t)$ is finite, being balanced by a non-zero $\partial E(k,t)/\partial t$. Thus condition (8.2) shows that Kolmogorov's similarity law holds under a weaker condition than the original one.

Recently, the energy transfer function $T(k)$ was measured by Helland, Van Atta & Stegen (1977) at large Reynolds numbers such that the inertial-subrange spectrum $E(k) \propto k^{-\frac{5}{3}}$ exists over one or two decades of the wavenumber. On comparing their results for the two functions $E(k)$ and $T(k)$, they found that $T(k)$ takes finite negative values over the inertial subrange and concluded that $T(k) \equiv 0$ may be a sufficient condition for the existence of the inertial-subrange spectrum but that the converse is apparently not valid. This conclusion is in accordance with our finding stated above.

(ii) Next, it may be seen in the figures for large Reynolds numbers that the k^{-1} spectrum always occurs in the neighbourhood of the wavenumber at which the energy transfer function $T(k,t)$ changes its sign, or in other words, in the range where

$$|T(k,t)| \ll D(k,t). \tag{8.3}$$

This is in perfect accord with the fact that the k^{-1} spectrum has been derived as an asymptotic solution of the equation

$$T(k,t) = 0 \tag{8.4}$$

for very large Reynolds numbers and times (Tatsumi 1960). Hence, according to the present theory, the k^{-1} spectrum must exist since the energy transfer function $T(k,t)$, which satisfies the condition

$$\int_0^\infty T(k,t)\,dk = 0,$$

must change sign somewhere. It should be remembered, however, that this conclusion is dependent upon the particular form of $T(k,t)$ in the present approximation given by (4.23) and (4.25). Since the wavenumber range for the k^{-1} spectrum seems to belong to the k_2 range, it is quite possible that the above conclusion would be modified by taking into account higher-order approximations.

(iii) Lastly, it is apparent from all the figures that the exponential spectrum of the form (6.1) occurs in the wavenumber range in which the energy transfer is nearly balanced by the energy dissipation:

$$T(k,t) \simeq D(k,t). \tag{8.5}$$

This situation is substantially different from that for weak turbulence, where the nonlinear transfer of energy is negligibly small, so that the energy dissipation is

balanced by the attenuation of the spectrum. The spectral form corresponding to such weak turbulence is the well-known viscous spectrum

$$E(k,t) \propto \exp(-2\nu k^2 t), \tag{8.6}$$

which was shown to appear in the final period of decay by Batchelor & Townsend (1948). The present result for turbulence of not very small Reynolds number shows that a spectrum of the type (8.6) does not occur even in the highest wavenumber range, where the energy density is quite low. Thus the asymptotic behaviour of turbulence at high wavenumbers should be accounted for by condition (8.5) instead of the linearized theory of weak turbulence.

8.2. *Similarity law of decay process*

In this subsection we shall develop a theory of the decay process of turbulence at large Reynolds numbers by using the characteristic features of the present numerical results and Kolmogorov's similarity law for the universal wavenumber range. The similarity law for the spectrum $E(k,t)$ in the energy-containing range and the inertial subrange may be summarized as follows.

(i) Throughout the energy-containing range and the inertial subrange the spectrum takes an inviscid similar form

$$E(k,t)/E_0 = \tau^{-\beta_1} F_1(\kappa/\tau^{\delta_1}). \tag{8.7}$$

(ii) In the lowest wavenumber part of the energy-containing range the spectrum (8.7) tends to

$$E(k,t)/E_0 = A_a \kappa^a, \tag{8.8}$$

where A_a and a are non-dimensional constants.

(iii) In the inertial subrange the spectrum (8.7) takes the form

$$E(k,t)/E_0 = B\tau^{-\beta_1+\frac{5}{3}\delta_1}\kappa^{-\frac{5}{3}}, \tag{8.9}$$

where B is a non-dimensional constant.

It was shown in § 8.1 that Kolmogorov's similarity law is applicable to the universal range of the decaying turbulence under consideration. Thus the spectrum in this range is expressed in Kolmogorov's similar form as

$$E(k,t) = \nu^{\frac{5}{4}}\epsilon(t)^{\frac{1}{4}} G(k/(\epsilon(t)/\nu^3)^{\frac{1}{4}}), \tag{8.10}$$

where the energy dissipation $\epsilon(t)$ is in this context a function of time and G is a non-dimensional function. In the inertial subrange the spectrum (8.10) takes the form

$$E(k,t) = K\epsilon(t)^{\frac{2}{3}}k^{-\frac{5}{3}}, \tag{8.11}$$

where K is a non-dimensional constant. Obviously, (8.11) is identical with the other expression for the inertial-subrange spectrum (8.9).

If the energy of the turbulence $\mathscr{E}(t)$ decays in time according to the relation

$$\mathscr{E}(t) \propto t^{-b}, \tag{8.12}$$

b being a constant, then the energy dissipation $\epsilon(t)$ changes in time according to

$$\epsilon(t) = -d\mathscr{E}(t)/dt \propto t^{-(b+1)}. \tag{8.13}$$

Now, if we suppose that the extensions of the lines given by (8.8) and (8.11) on a logarithmic graph intersect at the wavenumber k_s and denote $E(k_s, t)$ by E_s, then

$$E_s = A_a k_s^a = K\epsilon(t)^{\frac{2}{3}} k_s^{-\frac{5}{3}}.$$

Hence, in view of (8.13),

$$\left.\begin{aligned} k_s &\propto \epsilon(t)^{2/(3a+5)} \propto t^{-2(b+1)/(3a+5)}, \\ E_s &\propto t^{-2a(b+1)/(3a+5)}. \end{aligned}\right\} \tag{8.14}$$

Since the intersection point is completely determined by the spectrum (8.7), the variation of its abscissa and ordinate in time must obey the same similarity law as (8.7). Thus, comparing (8.7) and (8.14), we obtain

$$\beta_1 = 2a(b+1)/(3a+5), \quad \delta_1 = -2(b+1)/(3a+5). \tag{8.15}$$

Substitution from (8.15) into (8.7) yields

$$\begin{aligned} \mathscr{E}(t) = \int_0^\infty E(k,t)\,dk &= E_0 k_0 \tau^{-\beta_1+\delta_1} \int_0^\infty F_1(\xi)\,d\xi \\ &\propto t^{-2(a+1)(b+1)/(3a+5)}. \end{aligned} \tag{8.16}$$

Comparison of (8.16) with (8.12) gives

$$b = 2(a+1)/(a+3), \tag{8.17}$$

and hence, from (8.15),

$$\beta_1 = 2a/(a+3), \quad \delta_1 = -2/(a+3). \tag{8.18}$$

The values of β_1 and δ_1 thus obtained for cases I ($a = 2$) and II ($a = 4$) are given in table 1 together with the values $\alpha_1 = \gamma_1 = 0$ already assumed in (8.7). The agreement of these values with those from direct numerical calculation seems perfect, and this indicates that the similarity law (8.7) is satisfied by our numerical solutions with good accuracy.

The general law of the energy decay for an arbitrary a is obtained from (8.12) and (8.17) as

$$\mathscr{E}(t) \propto t^{-2(a+1)/(a+3)}, \tag{8.19}$$

so that, from (8.13),

$$\epsilon(t) \propto t^{-(3a+5)/(a+3)}. \tag{8.20}$$

For the special cases I and II, (8.19) gives

$$\text{(I)} \quad \mathscr{E}(t) \propto t^{-\frac{6}{5}} = t^{-1\cdot 2}, \tag{8.21}$$

$$\text{(II)} \quad \mathscr{E}(t) \propto t^{-\frac{10}{7}} = t^{-1\cdot 43}. \tag{8.22}$$

These results are again in agreement with (7.3) and (7.4) respectively.

The energy decay law (8.22) was first derived by Kolmogorov (1941*b*) from assumptions essentially equivalent to (8.7), (8.8) and (8.11) and re-derived by Comte-Bellot & Corrsin (1966) through a procedure similar to the present one but using a two-range model of the spectrum consisting of (8.8) and (8.11). It should be emphasized in this connexion that the existence of the inviscid similarity (8.7) is vital to deriving the energy decay law. Such an overall similarity is of a quite different nature from Kolmogorov's (1941*a*) similarity for the universal range and was actually introduced by Kolmogorov as an independent assumption originally due to von Kármán & Howarth

(1938). Comte-Bellot & Corrsin avoided assumption of such a similarity by taking a special two-range model of the spectrum, but nevertheless it must be proved that there exists a spectrum connecting smoothly these two ranges and satisfying an overall similarity before their result may be taken to be realistic. As we have seen in § 7, such a similar spectrum covering the energy-containing range and the inertial subrange has actually been provided by the present numerical results and this gives strong support to the validity of the energy decay law (8.19) with (8.21) and (8.22).

The constant A_4 is related to the so-called Loitsiansky integral

$$A_4 = \frac{1}{3\pi} u(t)^2 \int_0^\infty r^4 f(r,t)\, dr, \tag{8.23}$$

where $u(t)$ is the root-mean-square velocity and $f(r,t)$ is the longitudinal correlation function. It was shown by Proudman & Reid (1954) for turbulence with zero fourth-order cumulants that A_4 is not invariant, and the same result was obtained by Batchelor & Proudman (1956) for general homogeneous turbulence. Thus the above derivation of the law (8.22) based on the invariance of A_4 seems doubtful. Nevertheless, the deviation from invariance is found to be very small in the numerical results of the present theory as may be seen from the behaviour of the case II spectra at very low wavenumbers which are shown in figures 2 (*b*) and (*d*). Thus the energy decay law (8.22) is in fact valid with sufficient accuracy.

On the other hand, it was found by Birkhoff (1954) that the coefficient A_2, which is related to the correlation function by

$$A_2 = u(t)^2 \lim_{r\to\infty} \{r^3 f(r,t)\}, \tag{8.24}$$

is invariant. Following Kolmogorov, or Comte-Bellot & Corrsin, but replacing the invariance of A_4 by that of A_2, Saffman (1967) derived the decay law (8.21). The invariance of A_2 is perfectly confirmed by the behaviour of the case I spectra at very low wavenumbers as shown in figures 2 (*a*) and (*c*). Thus it may be said that the energy decay law (8.21) has a stronger physical basis than (8.22).

Now that we have established the relationship (8.20), we can derive the similarity form of the spectrum (7.1) from Kolmogorov's similarity form (8.10) as follows:

$$E(k,t)/E_0 = R^{-\frac{5}{4}} T^{-(3a+5)/4(a+3)} F_2(\kappa/(R^{\frac{3}{4}} T^{-(3a+5)/4(a+3)})). \tag{8.25}$$

The values of the exponents for cases I and II are given in table 2. The agreement with the values from direct numerical work is excellent.

9. Miscellaneous statistical characteristics

Once the energy spectrum function $E(k,t)$ and the energy transfer function $T(k,t)$ have been obtained numerically, various statistical characteristics of the turbulence may immediately be derived from these data.

9.1. *Decay of energy*

The energy of the turbulence $\mathscr{E}(t)$ is computed from numerical data on the spectrum $E(k,t)$ using (4.6) and the result is shown graphically in figures 7 (*a*) and (*b*) for cases I and II respectively. The existence of the initial and similarity periods may be clearly observed in the curves for large Reynolds numbers ($R \geqslant 100$) for both cases.

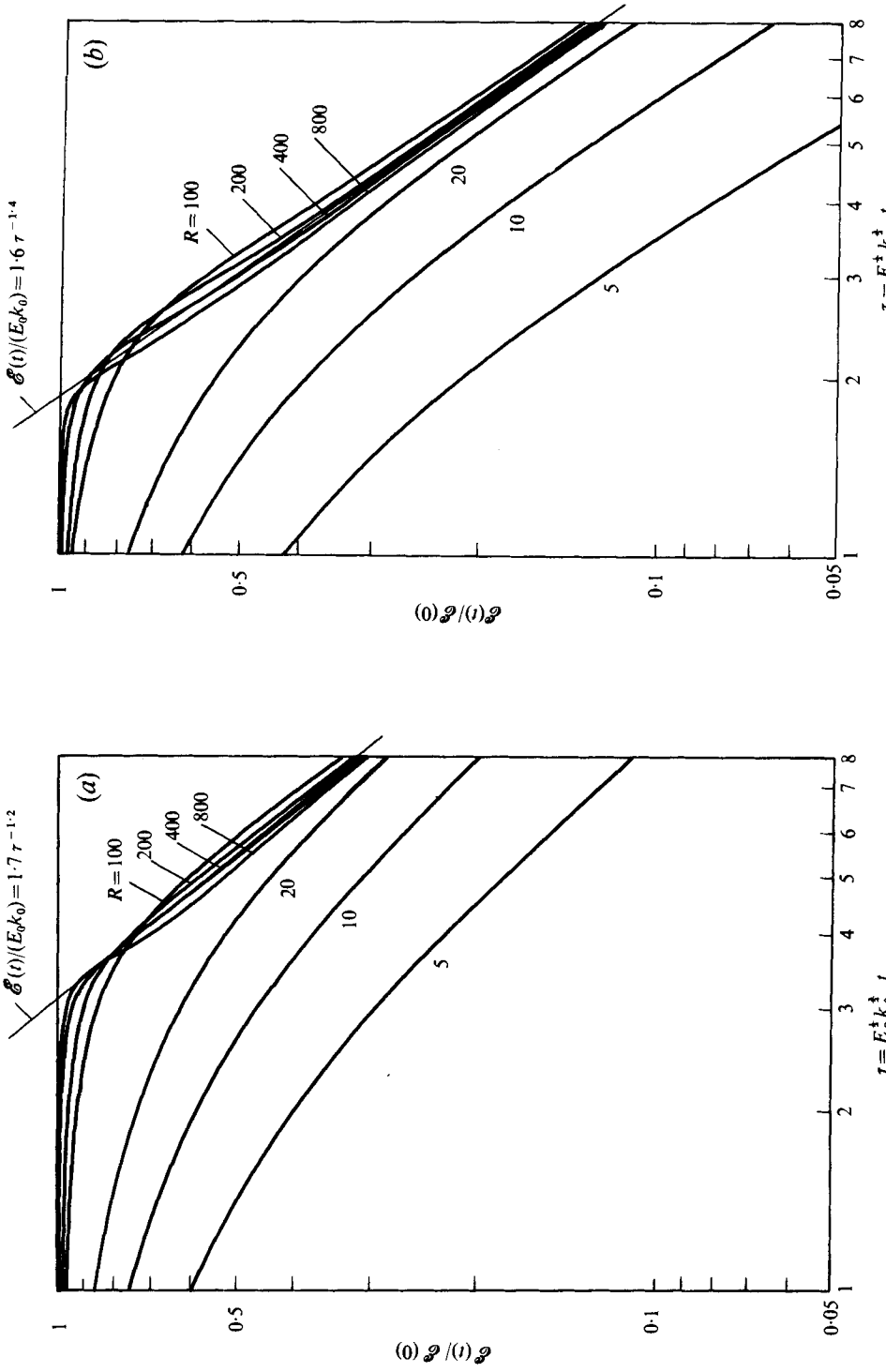

FIGURE 7. The decay of the energy $\mathscr{E}(t)$. (a) Case I, $\mathscr{E}(0)/E_0k_0 = 0{\cdot}4431$. (b) Case II, $\mathscr{E}(0)/E_0k_0 = 0{\cdot}6647$.

In the initial period, roughly corresponding to $0 \leqslant \tau \leqslant 3$ for case I and $0 \leqslant \tau \leqslant 2$ for case II, $\mathscr{E}(t)$ does not change appreciably. Thus the nonlinear transfer of energy to higher wavenumbers is carried out without changing the total energy in this period.

In the similarity period, roughly corresponding to $\tau \geqslant 4$ for case I and $\tau \geqslant 3$ for case II, on the other hand, $\mathscr{E}(t)$ decays in time according to a power law in each case. The optimum-fit straight lines for the curves for $R \geqslant 200$ gives the following law of the energy decay for each case:

$$\text{(I)} \quad \mathscr{E}(t)/(E_0 k_0) = 1{\cdot}7\tau^{-1{\cdot}2}, \tag{9.1}$$

$$\text{(II)} \quad \mathscr{E}(t)/(E_0 k_0) = 1{\cdot}6\tau^{-1{\cdot}4}. \tag{9.2}$$

These results are in perfect agreement with (7.3) and (7.4), which were derived from consideration of similarity of the spectrum.

The available experimental data on the energy decay law for grid-generated turbulence are not decisive with respect to the numerical value of the exponent. In early studies the exponent was taken to be -1 (see Batchelor 1953, §7·1) but later experiments gave values ranging between $-1{\cdot}0$ and $-1{\cdot}4$ (see table 1 of Comte-Bellot & Corrsin 1966). In most experiments the exponent cannot be determined uniquely since the energies associated with the velocity components in the streamwise and transverse directions obey slightly different decay laws. Comte-Bellot & Corrsin (1966) produced almost isotropic turbulence with weak contraction of the wind tunnel and obtained an exponent of $-1{\cdot}25$, which is fairly close to that in (9.1). On the other hand, a group of more recent measurements by Ling & Wan (1972), Gad-el-Hak & Corrsin (1974) and Tassa & Kamotani (1975) give exponents ranging between $-1{\cdot}30$ and $-1{\cdot}35$, which are closer to (9.2) than (9.1).

9.2. *Kolmogorov's constant*

The rate of energy dissipation $\epsilon(t)$ is immediately obtained from (9.1) and (9.2) as

$$\text{(I)} \quad \epsilon(t)/(E_0^{\frac{3}{2}} k_0^{\frac{5}{2}}) = 2{\cdot}0\tau^{-2{\cdot}2}, \tag{9.3}$$

$$\text{(II)} \quad \epsilon(t)/(E_0^{\frac{3}{2}} k_0^{\frac{5}{2}}) = 2{\cdot}2\tau^{-2{\cdot}4}. \tag{9.4}$$

By substituting these relations into the spectral form (8.11), we can calculate Kolmogorov's constant K. The values of $E(k,t)$ are taken directly from the curves of the spectrum at $\tau = 5$, 6, 7 and 8 for $R = 200$, 400 and 800. The values of K thus obtained vary slightly with Reynolds number and time but lie in the following ranges:

$$\text{(I)} \quad K = 0{\cdot}60 \sim 0{\cdot}62, \tag{9.5}$$

$$\text{(II)} \quad K = 0{\cdot}56 \sim 0{\cdot}59. \tag{9.6}$$

It should be noted that these values of K are nearly equal for cases I and II, showing that the small-scale structure of turbulence at large Reynolds numbers is essentially independent of its large-scale structure.

Kolmogorov's constant K has been measured by several experimentalists in various types of turbulence. The measurements by Grant *et al.* (1962) in tidal streams gave $K = 1{\cdot}44$ and those due to Wyngaard & Pao (1972) in atmospheric winds the slightly higher value $K = 1{\cdot}7$. In laboratory turbulence, Gibson (1962, 1963) obtained $K = 1{\cdot}57$ (on the axis) and 1·62 (off the axis) in a round jet, Gibson & Schwarz (1963) obtained $K = 1{\cdot}34 \pm 0{\cdot}06$ in grid turbulence and Schedvin *et al.* (1974) obtained $K = 1{\cdot}47 \pm 0{\cdot}18$

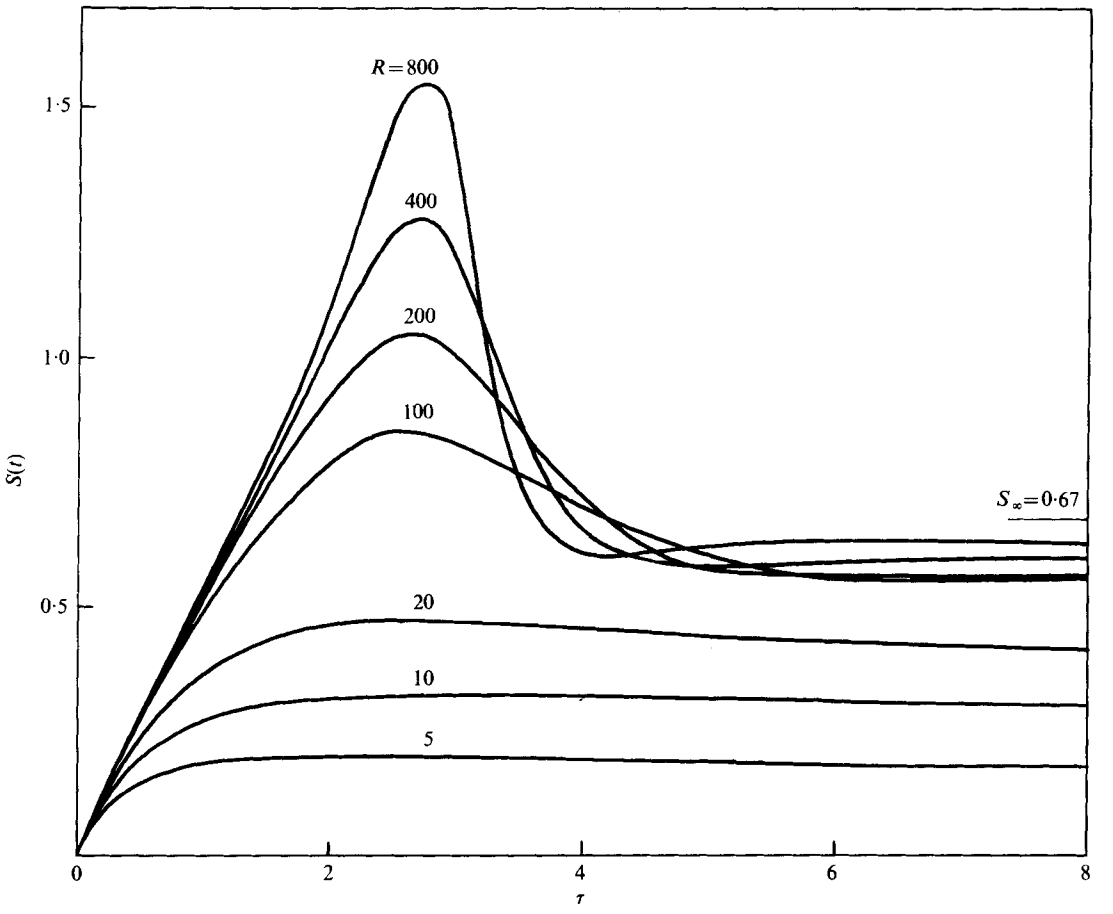

FIGURE 8 (*a*). For legend see facing page.

in grid turbulence. The measurements by Kistler & Vrebalovich (1966) in grid turbulence yielded $K = 2{\cdot}1 \sim 2{\cdot}7$, but these high values of K were questioned by later authors since their spectra are not consistent with the general trend of spectra at increasing Reynolds numbers (see Schedvin *et al.* 1974).

The theoretical values of K given by (9.5) and (9.6) are considerably smaller than these measured values. We have no definite explanation for this discrepancy, but it may be due to the overestimation of the energy dissipation ϵ in the present theory. The value of ϵ is increased by the presence of the k^{-1} spectrum, which has not been observed experimentally. If, as mentioned in §8.1, this part of the spectrum is modified at higher stages of approximation there is a possibility of obtaining smaller values of ϵ and consequently larger values of K.

9.3. *Skewness of velocity derivative*

The skewness $S(t)$ of the velocity derivative defined by (5.11) gives a non-dimensional measure of the strength of the vorticity production. Since $S(t)$ is expressed as an integral of $E(k,t)$ weighted towards higher wavenumbers, it reflects the behaviour of the spectrum in the universal range, or the small-scale structure of turbulence. Thus

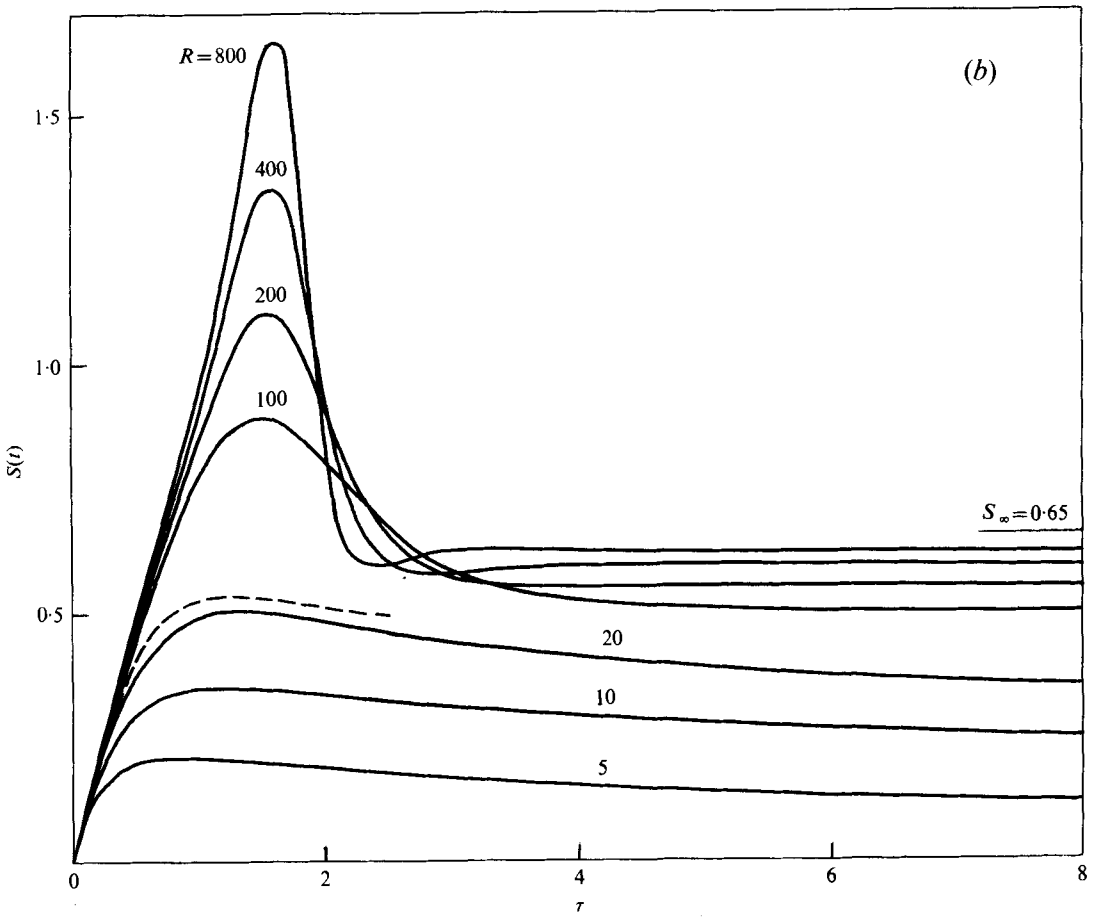

FIGURE 8. The skewness $S(t)$ of the velocity derivative. (*a*) Case I. (*b*) Case II; — —, numerical experiment by Orszag & Patterson (1972) for $R = 21$.

$S(t)$ furnishes us with information on turbulence complementary to that from the energy $\mathscr{E}(t)$, which represents the behaviour of the spectrum in the energy-containing range, or the large-scale structure of turbulence.

$S(t)$ is calculated by substituting numerical values of $E(k,t)$ and $T(k,t)$ into (5.11) and the result is shown graphically in figures 8 (*a*) and (*b*) for cases I and II respectively. The initial value $S(0)$ is identically zero for both cases according to the initial condition (5.7). At small Reynolds numbers, $S(t)$ increases gradually in time to an asymptotic value $S_\infty = S(\infty)$. At large Reynolds numbers, on the other hand, it overshoots once and then returns rapidly to an asymptotic value S_∞. Roughly speaking, $S(t)$ undergoes overshooting in the initial period and remains constant during the similarity period.

The asymptotic value S_∞ increases monotonically with Reynolds number and seems to approach the following values in the limit of infinite Reynolds number:

$$\text{(I)} \quad S_\infty = 0{\cdot}67, \tag{9.7}$$

$$\text{(II)} \quad S_\infty = 0{\cdot}65. \tag{9.8}$$

The agreement of the above values of S_∞ for cases I and II makes a clear contrast to the disagreement of the energy decay laws $\mathscr{E}(t)$ for the two cases, giving further evidence of a universality of the small-scale structure of turbulence independent of its large-scale structure.

Earlier measurements of $S(t)$ in grid-generated turbulence made by Batchelor & Townsend (1947, 1949) and Stewart (1951) give values in the range 0·3–0·5, which are compatible with the present results at relatively small Reynolds numbers, but no further comparison is possible owing to the lack of other statistical data related to the measured values. Later measurements by Uberoi (1963) show that $S(t)$ is nearly constant in time with a value of about 0·54. This value is fairly close to the present results for $R = 100$ or 200 for either case. Taking into account general features of the spectrum and the energy decay law, Uberoi's measurement seems to correspond to our case I at $R = 100$.

Orszag & Patterson (1972) carried out numerical experiments on decaying isotropic turbulence starting from the initial condition corresponding to case II. The curves of $S(t)$ derived from the calculations with $R = R_\lambda(0) = 21$, 35 and 42 [see (5.15)] are found to be identical within statistical fluctuations. The curve for $R = 21$, which is plotted in figure 8(*b*) for comparison, shows striking agreement with the present curve for $R = 20$. The average of S_∞ for the above values of $R_\lambda(0)$ is about 0·48, roughly in accordance with our result for case II.

Measurements of stationary atmospheric turbulence made by Wyngaard & Pao (1972) give the value of $S(t) = S_\infty$ to be in the range 0·70–0·85. These values are considerably larger than the present values given by (9.7) and (9.8) even taking into account the extremely large values $R_\lambda = 10^3 \sim 10^4$ for the measurements.

9.4. *Microscale*

The microscale $\lambda(t)$ defined by (5.12) gives another parameter representing the small-scale structure of turbulence. The value of $\lambda(t)$ is obtained by substituting numerical values of $E(k,t)$ into (5.12) and the result is shown graphically in figures 9(*a*) and (*b*) for cases I and II respectively. At small Reynolds numbers $\lambda(t)$ increases monotonically in time, whereas at large Reynolds numbers it decreases rapidly from its initial value to a minimum and then increases almost proportionally with time. Roughly speaking, its rapid decrease at large Reynolds numbers takes place in the initial period and its linear growth occurs during the similarity period.

By making use of (4.6) and (4.22), the microscale $\lambda(t)$ may be expressed in terms of the energy $\mathscr{E}(t)$ as

$$\lambda(t)^2 = -10\nu\mathscr{E}(t)\,(d\mathscr{E}(t)/dt)^{-1}. \tag{9.9}$$

Substituting (9.1) and (9.2) into (9.9) we obtain the following similarity laws for the microscale:

$$\text{(I)} \quad \lambda(t)^2 = 8{\cdot}3\tau/(Rk_0^2) = 8{\cdot}3\nu t, \tag{9.10}$$

$$\text{(II)} \quad \lambda(t)^2 = 7{\cdot}1\tau/(Rk_0^2) = 7{\cdot}1\nu t. \tag{9.11}$$

It may be seen in figures 9(*a*) and (*b*) that these similarity laws are satisfied fairly well by the curves for $R \geqslant 200$ in both cases.

If we substitute the expression (8.19) for $\mathscr{E}(t)$ into (9.9), we obtain the general formula for $\lambda(t)$ for arbitrary a as

$$\lambda(t)^2 = \frac{5(a+3)}{a+1}\frac{\tau}{Rk_0^2} = \frac{5(a+3)}{a+1}\nu t. \tag{9.12}$$

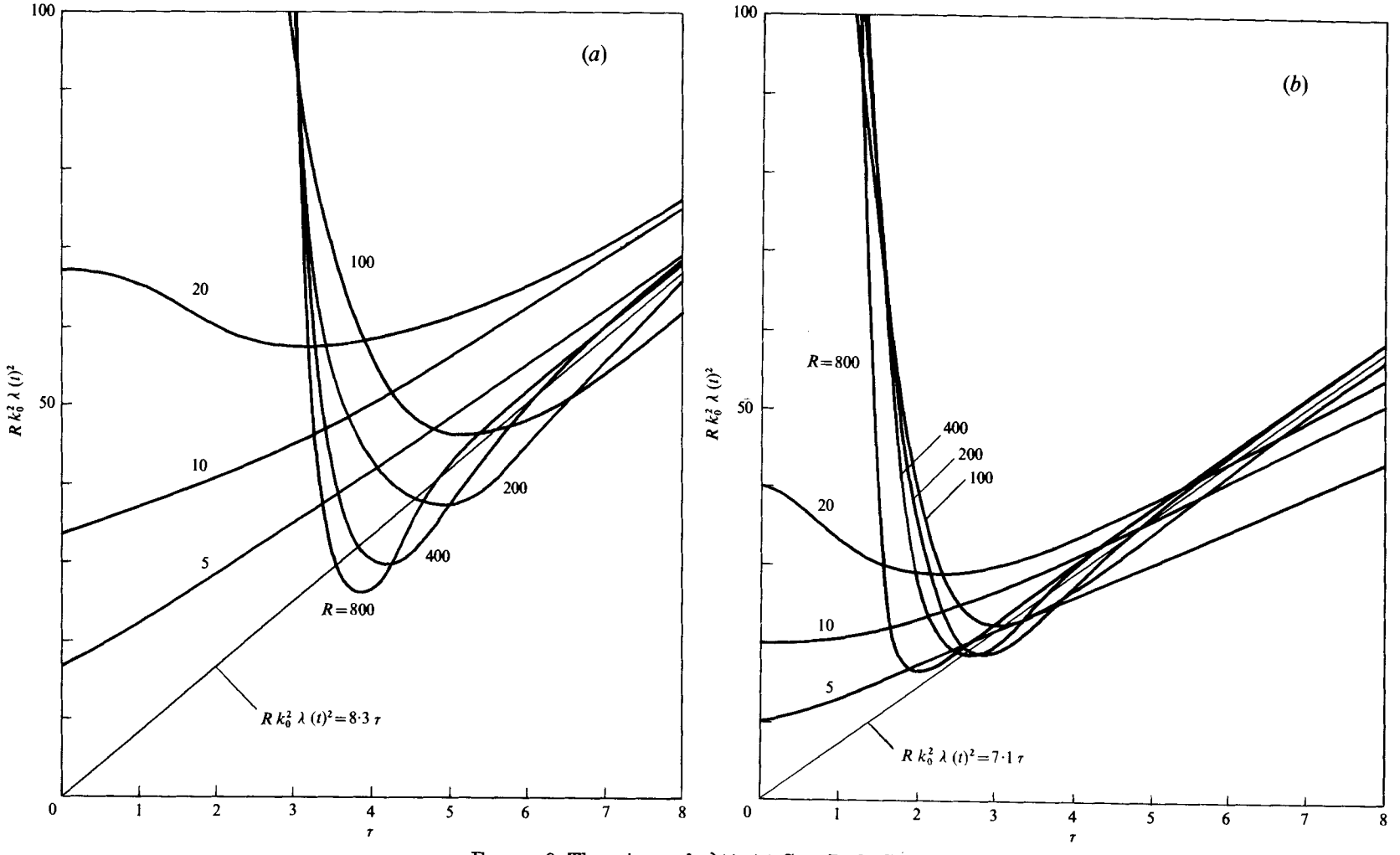

FIGURE 9. The microscale $\lambda(t)$. (*a*) Case I. (*b*) Case II.

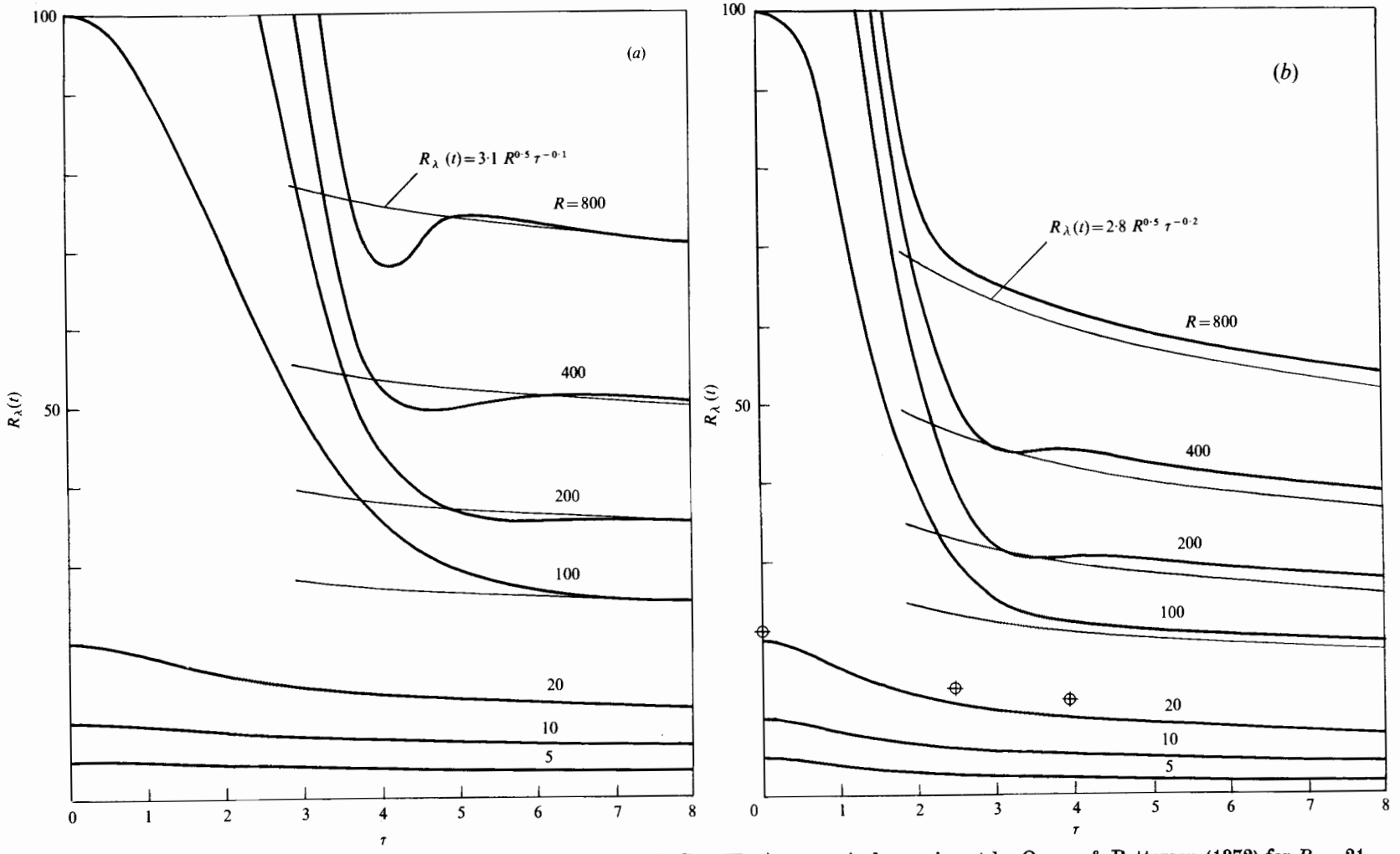

FIGURE 10. The microscale Reynolds number $R_\lambda(t)$. (*a*) Case I. (*b*) Case II; $\oplus$, numerical experiment by Orszag & Patterson (1972) for $R = 21$.

This formula gives coefficients of $\frac{2}{3}5 \fallingdotseq 8{\cdot}3$ for case I and 7 for case II, which are exactly and nearly equal to those in (9.10) and (9.11) respectively.

9.5. *Microscale Reynolds number*

The Reynolds number R as defined by (5.1) is based on E_0 and k_0, which are related to the initial conditions and therefore not suitable for characterizing the state of non-stationary turbulence at an arbitrary time. For such a purpose it is more convenient to use the microscale Reynolds number $R_\lambda(t)$ defined by (5.14). The variation of $R_\lambda(t)$ in time is easily obtained from the data on $\mathscr{E}(t)$ ($= \frac{3}{2}u(t)^2$) and $\lambda(t)$ and is shown graphically in figures 10(*a*) and (*b*) for cases I and II respectively.

At small values of R, the microscale Reynolds number $R_\lambda(t)$ decreases gradually and monotonically from its initial value $R_\lambda(0)$ ($\fallingdotseq R$). At large R, on the other hand, it decreases very rapidly in the initial period and rather slowly in the similarity period. The asymptotic behaviour of $R_\lambda(t)$ for large R and τ is easily derived from equations (9.1) and (9.2) for $\mathscr{E}(t)$ and equations (9.10) and (9.11) for $\lambda(t)$ as follows:

$$\text{(I)} \quad R_\lambda(t) = 3{\cdot}1R^{0{\cdot}5}\tau^{-0{\cdot}1}, \tag{9.13}$$

$$\text{(II)} \quad R_\lambda(t) = 2{\cdot}8R^{0{\cdot}5}\tau^{-0{\cdot}2}. \tag{9.14}$$

The agreement of the numerical curves with these asymptotic curves seems fairly good in the similarity period for both cases.

Numerical values of $R_\lambda(t)$ due to Orszag & Patterson's numerical experiment for $R = 21$ are plotted in figure 10(*b*) for comparison. The agreement with the present result for $R = 20$ is again satisfactory. Unlike the numerical experiments the experimental data on grid-generated turbulence are usually specified in terms of the so-called mesh Reynolds number

$$R_M = UM/\nu \tag{9.15}$$

and the downstream distance x/M, where U is the wind velocity and M is the mesh length of the grid. However, the mesh Reynolds number R_M, being related only to the initial state of the grid turbulence, gives no information about the state of downstream turbulence unless supplemented by other statistical data. It is this lack of experimental information that has sometimes hindered immediate comparison of theoretical and experimental results. In view of the fact that the intensity $u(t)$ and the microscale $\lambda(t)$ of turbulence are both very standard quantities in turbulence measurements, it may not be difficult to record the value of R_λ for all statistical data on turbulence. Undoubtedly, such a custom will ease the theoretical treatment of the experimental results considerably.

9.6. *Self-preservation of energy spectrum*

Since the root-mean-square velocity $u(t)$ and the microscale $\lambda(t)$ are statistical quantities readily measurable by standard experimental techniques it is natural that these quantities have been used sometimes for testing the similarity or self-preservation of the measured energy spectrum. Such a test was made by Stewart & Townsend (1951) for grid-generated turbulence and the measured spectra were found to satisfy approximately self-preservation in this sense. Though sufficient data for calculating R_λ were not given in their paper, the measurements by Batchelor & Townsend (1947), which seem to have been carried out in approximately the same conditions, give an R_λ of about 20. According to the relation between R_λ and R given in figure 10(*b*) for case II,

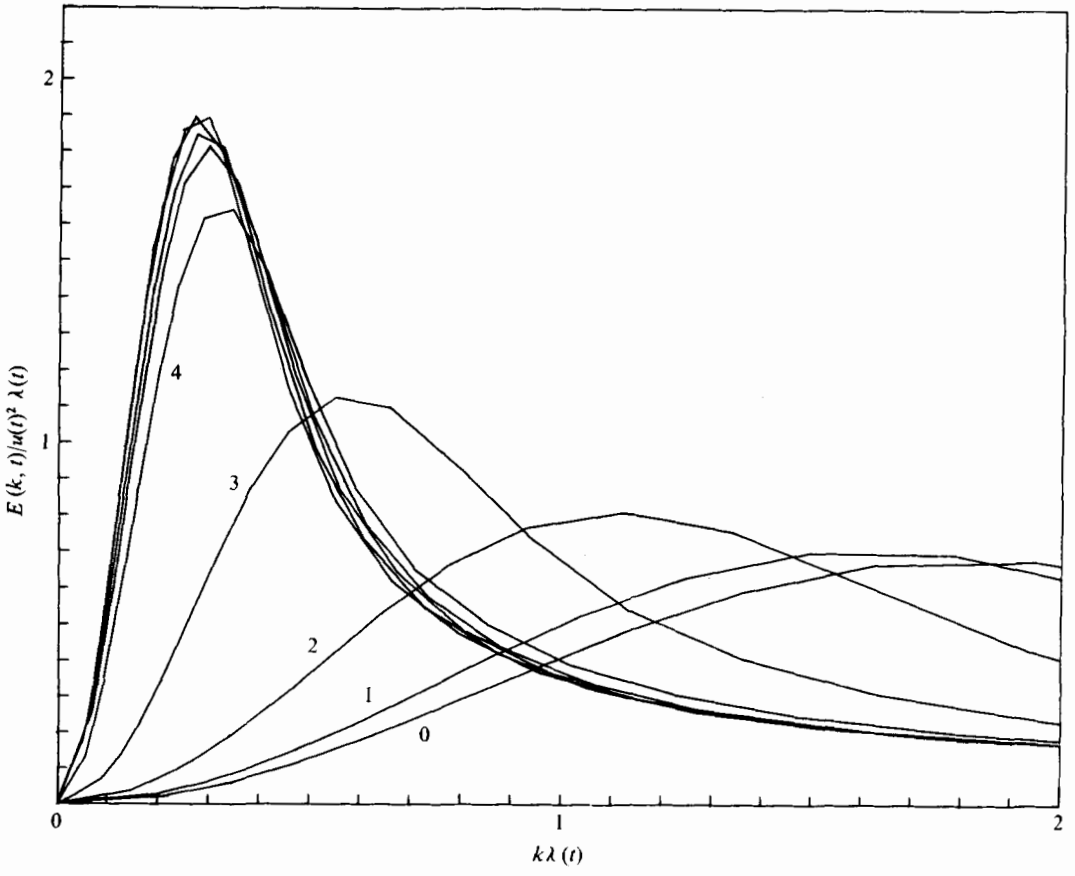

FIGURE 11 (*a*). For legend see facing page.

this value of R_λ corresponds to an R of about 100. In fact, the curves for $R = 200$ for case II shown in figure 11 (*b*) seem to have the closest resemblance to the measured curves of Stewart & Townsend.

Generally speaking, the spectra normalized with respect to $u(t)$ and $\lambda(t)$ coincide with each other fairly well, showing the validity of self-preservation in this sense, but the coincidence is less satisfactory for the curves for case II. These results can be explained if we consider the inviscid similarity of the spectrum in the energy-containing range and the inertial subrange.

It immediately follows from (9.1), (9.2), (9.10) and (9.11) that the scale of the energy spectrum in the above normalization changes in time as

$$\text{(I)} \quad u^2\lambda \propto t^{-0.7}, \qquad \text{(II)} \quad u^2\lambda \propto t^{-0.9}.$$

On the other hand, according to the inviscid similarity (7.1) with the exponents given in table 1, the magnitude of the spectrum must change in time as

$$\text{(I)} \quad t^{-\beta_1} = t^{-0.8}, \qquad \text{(II)} \quad t^{-\beta_1} = t^{-1.1}.$$

Thus it is evident from comparison of the above results that the self-preservation with respect to $u(t)$ and $\lambda(t)$ is nearly equivalent to the inviscid similarity for case I but is less accurately so for case II.

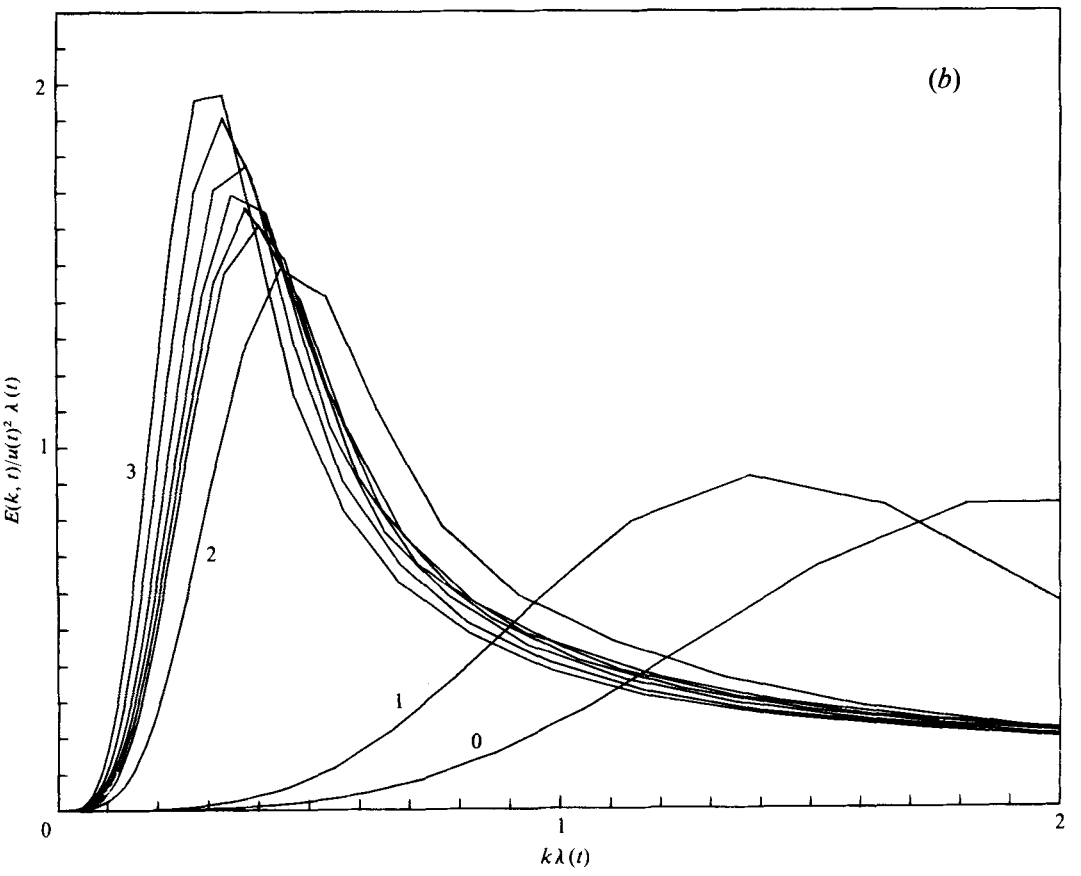

FIGURE 11. The self-preservation of the energy spectrum function $E(k, t)$ for $R = 200$. (*a*) Case I. (*b*) Case II.

The same trend is also observed for the scale of the wavenumber since λ^{-1} changes in time as

$$\text{(I), (II)} \quad \lambda^{-1} \propto t^{-0.5},$$

while according to inviscid similarity, the scale of the wavenumber must change in time as

$$\text{(I)} \quad t^{\delta_1} = t^{-0.4}, \qquad \text{(II)} \quad t^{\delta_1} = t^{-0.3}.$$

Here again the discrepancy in the exponents is larger in case II than in case I.

Thus it may be concluded that the self-preservation of the energy spectrum $E(k, t)$ with respect to the root-mean-square velocity $u(t)$ and the microscale $\lambda(t)$ is satisfied only approximately and that the normalization of the spectrum would be more legitimate if done by using the inviscid similarity law given by (7.1) and table 1.

10. Summary and discussion

The statistical properties of turbulence derived from the multiple-scale cumulant expansion method may be summarized as follows. At large Reynolds numbers the decaying turbulence assumes, after an initial time period, a similarity state in which it is governed by simple similarity laws dependent upon only a few parameters. The statistical laws stated below are effective in this similarity period.

The energy spectrum $E(k,t)$ has an inertial subrange in which it is expressed as in (8.11) with a K of about 0·6, and the extent of this subrange increases indefinitely with the Reynolds number R.

The spectrum in the energy-containing and inertial ranges satisfies an inviscid similarity law (8.7), so that the energy $\mathscr{E}(t)$ decays in time according to (9.1) or (9.2), at a rate independent of the viscosity.

The spectrum in and beyond the inertial subrange has a universal form which is independent of its low wavenumber structure and consistent with Kolmogorov's similarity law (8.10). The universal spectrum takes the following forms successively with increasing wavenumber: (i) the inertial-subrange spectrum (7.6) or (7.7), (ii) the k^{-1} spectrum (7.8) or (7.9) and (iii) the exponential spectrum (7.10) or (7.11).

The energy decay law can be generalized as (8.19), which includes (9.1) and (9.2) as special cases.

The skewness $S(t)$ of the velocity derivative remains nearly constant in time and its value increases with R to a limit of about 0·7.

The microscale $\lambda(t)$ increases in time according to the general formula (9.12), which includes (9.10) and (9.11) as special cases.

The microscale Reynolds number $R_\lambda(t)$ decreases very slowly in time according to (9.13) or (9.14) with a coefficient proportional to $R^{\frac{1}{2}}$.

The spectrum $E(k,t)$ normalized with respect to the root-mean-square velocity $u(t)$ and the microscale $\lambda(t)$ is found to be approximately self-preserving in time. For the purpose of normalization of the spectrum, however, it would be preferable to use the inviscid similarity law (8.7), which is exactly satisfied by the spectrum.

Most of the statistical results described above are consistent with existing experimental data at large Reynolds numbers. Probably the only prominent disagreement between the present result and measurements lies in the numerical value of Kolmogorov's constant K, since our value of about 0·6 is considerably smaller than the measured values, which lie in the range 1·4–1·7.This discrepancy, however, arises from the difference in the viscous dissipation, which is largely influenced by the spectrum at higher wavenumbers. It is well known that accurate measurement of the spectrum is hampered by several experimental difficulties at high wavenumbers. On the other hand, this part of the spectrum may possibly be modified by taking into account higher-order approximations. Thus the resolution of this discrepancy remains a subject for future work.

The authors wish to express their hearty gratitude to Dr Takuji Kawahara for helpful advice and discussions and to Mr Masaharu Kouno for assistance with numerical work. This work was partially supported by Grants-in-Aid for Scientific Research (A) 034018, 064105 and 154091 from the Ministry of Education.

REFERENCES

BATCHELOR, G. K. 1953 *The Theory of Homogeneous Turbulence*. Cambridge University Press.

BATCHELOR, G. K. 1959 Small-scale variation of convected quantities like temperature in turbulent fluid. 1. General discussion and the case of small conductivity. *J. Fluid Mech.* **5**, 113–133.

BATCHELOR, G. K. & PROUDMAN, I. 1956 The large-scale structure of homogeneous turbulence. *Phil. Trans. Roy. Soc.* A **248**, 369–405.

BATCHELOR, G. K. & TOWNSEND, A. A. 1947 Decay of vorticity in isotropic turbulence. *Proc. Roy. Soc.* A **191**, 534–550.

BATCHELOR, G. K. & TOWNSEND, A. A. 1948 Decay of turbulence in the final period. *Proc. Roy. Soc.* A **194**, 527–543.

BATCHELOR, G. K. & TOWNSEND, A. A. 1949 The nature of turbulent motion at large wave-numbers. *Proc. Roy. Soc.* A **199**, 238–255.

BIRKHOFF, G. 1954 Fourier synthesis of homogeneous turbulence. *Comm. Pure Appl. Math.* **7**, 19–44.

BOGOLIUBOV, N. N. 1962 *Studies in Statistical Mechanics*, vol. 1 (ed. J. de Boer & G. E. Uhlenbeck). North-Holland.

COMTE-BELLOT, G. & CORRSIN, S. 1966 The use of a contraction to improve the isotropy of grid-generated turbulence. *J. Fluid Mech.* **25**, 657–682.

EDWARDS, S. F. 1964 The statistical dynamics of homogeneous turbulence. *J. Fluid Mech.* **18**, 239–273.

FRENKIEL, F. N. & KLEBANOFF, P. S. 1967 Higher-order correlations in a turbulent field. *Phys. Fluids* **10**, 507–520.

GAD-EL-HAK, M. & CORRSIN, S. 1974 Measurements of the nearly isotropic turbulence behind a uniform jet grid. *J. Fluid Mech.* **62**, 115–143.

GIBSON, M. M. 1962 Spectra of turbulence at high Reynolds number. *Nature*, **195**, 1281–1283.

GIBSON, M. M. 1963 Spectra of turbulence in a round jet. *J. Fluid Mech.* **15**, 161–173.

GIBSON, C. H. & SCHWARZ, W. H. 1963 The universal equilibrium spectra of turbulent velocity and scalar fields. *J. Fluid Mech.* **16**, 365–384.

GRANT, H. L., HUGHES, B. A., VOGEL, W. M. & MOILLIET, A. 1968 The spectrum of temperature fluctuations in turbulent flow. *J. Fluid Mech.* **34**, 423–442.

GRANT, H. L. & MOILLIET, A. 1962 The spectrum of a cross-stream component of turbulence in a tidal stream. *J. Fluid Mech.* **13**, 237–240.

GRANT, H. L., STEWART, R. W. & MOILLIET, A. 1962 Turbulence spectra from a tidal channel. *J. Fluid Mech.* **12**, 241–268.

HELLAND, K. N., VAN ATTA, C. W. & STEGEN, G. R. 1977 Spectral energy transfer in high Reynolds number turbulence. *J. Fluid Mech.* **79**, 337–359.

HERRING, J. R. 1965 Self-consistent-field approach to turbulence theory. *Phys. Fluids* **8**, 2219–2225.

HERRING, J. R. 1966 Self-consistent-field approach to nonstationary turbulence. *Phys. Fluids* **9**, 2106–2110.

HERRING, J. R. & KRAICHNAN, R. H. 1972 Comparison of some approximations for isotropic turbulence. In *Statistical Models and Turbulence. Lecture Notes in Physics*, vol. 12 (ed. M. Rosenblatt & C. Van Atta), pp. 148–194. Springer.

HOPF, E. 1952 Statistical hydromechanics and functional calculus. *J. Rat. Mech. Anal.* **1**, 87–123.

KÁRMÁN, T. VON & HOWARTH, L. 1938 On the statistical theory of isotropic turbulence. *Proc. Roy. Soc.* A **164**, 192–215.

KAWAHARA, T. 1968 A successive approximation for turbulence in the Burgers model fluid. *J. Phys. Soc. Japan* **25**, 892–900.

KISTLER, A. L. & VREBALOVICH, T. 1961 Grid turbulence at high Reynolds numbers. *Bull. Am. Phys. Soc.* **6**, 207.

KISTLER, A. L. & VREBALOVICH, T. 1966 Grid turbulence at large Reynolds numbers. *J. Fluid Mech.* **26**, 37–47.

KOLMOGOROV, A. N. 1941*a* The local structure of turbulence in incompressible viscous fluid for very large Reynolds numbers. *C. R. Acad. Sci. U.R.S.S.* **30**, 301–305.

KOLMOGOROV, A. N. 1941*b* On degeneration of isotropic turbulence in an incompressible viscous liquid. *C. R. Acad. Sci. U.R.S.S.* **31**, 538–540.

KOLMOGOROV, A. N. 1941*c* Dissipation of energy in the locally isotropic turbulence. *C. R. Acad. Sci. U.R.S.S.* **32**, 16–18.

KRAICHNAN, R. H. 1964 Approximations for steady-state isotropic turbulence. *Phys. Fluids* **7**, 1163–1168.

KRAICHNAN, R. H. 1971 An almost-Markovian Galilean-invariant turbulence model. *J. Fluid Mech.* **47**, 513–524.

LEITH, C. E. 1971 Atmospheric predictability and two-dimensional turbulence. *J. Atmos. Sci.* **28**, 145–161.

LING, S. C. & WAN, C. A. 1972 Decay of isotropic turbulence generated by a mechanically agitated grid. *Phys. Fluids* **15**, 1363–1369.

MALFLIET, W. P. M. 1969 A theory of homogeneous turbulence deduced from the Burgers equation. *Physica* **45**, 257–271.

MILLIONSHTCHIKOV, M. 1941 On the theory of homogeneous isotropic turbulence. *C. R. Acad. Sci. U.R.S.S.* **32**, 615–618.

MONIN, A. S. & YAGLOM, A. M. 1975 *Statistical Fluid Mechanics*, vol. 2. M.I.T. Press.

OGURA, Y. 1963 A consequence of the zero-fourth-cumulant approximation in the decay of isotropic turbulence. *J. Fluid Mech.* **16**, 38–41.

ORSZAG, S. A. 1970 Analytical theories of turbulence. *J. Fluid Mech.* **41**, 363–386.

ORSZAG, S. & PATTERSON, G. S. 1972 Numerical simulation of turbulence. In *Statistical Models and Turbulence. Lecture Notes on Physics*, vol. 12 (ed. M. Rosenblatt & C. Van Atta), pp. 127–147. Springer.

PAO, Y. H. 1965 Structure of turbulent velocity and scalar fields at large wavenumbers. *Phys. Fluids* **8**, 1063–1075.

PAO, Y. H. 1968 Transfer of turbulent energy and scalar quantities at large wavenumbers. *Phys. Fluids* **11**, 1371–1372.

PROUDMAN, I. & REID, W. H. 1954 On the decay of normally distributed and homogeneous turbulent velocity fields. *Phil. Trans. Roy. Soc.* A **247**, 163–189.

SAFFMAN, P. G. 1967 Note on decay of homogeneous turbulence. *Phys. Fluids* **10**, 1349.

SAFFMAN, P. G. 1968 In *Lectures on Homogeneous Turbulence. Topics in Nonlinear Physics* (ed. N. J. Zabusky), pp. 485–614. Springer.

SCHEDVIN, J., STEGEN, G. R. & GIBSON, C. H. 1974 Universal similarity at high grid Reynolds numbers. *J. Fluid Mech.* **56**, 561–579.

STEWART, R. W. 1951 Triple velocity correlations in isotropic turbulence. *Proc. Camb. Phil. Soc.* **47**, 146–147.

STEWART, R. W. & TOWNSEND, A. A. 1951 Similarity and self-preservation in isotropic turbulence. *Phil. Trans. Roy. Soc.* A **243**, 359–386.

TANAKA, H. 1969 0–5th cumulant approximation of inviscid Burgers turbulence. *J. Met. Soc. Japan* **47**, 373–383.

TANAKA, H. 1973 Higher order successive expansion of inviscid Burgers turbulence. *J. Phys. Soc. Japan* **34**, 1390–1395.

TASSA, Y. & KAMOTANI, Y. 1975 Experiments on turbulence behind a grid with jet injection in downstream and upstream direction. *Phys. Fluids* **18**, 411–414.

TATSUMI, T. 1955 Theory of isotropic turbulence with the normal joint-probability distribution of velocity. *Proc. 4th Japan Nat. Cong. App. Mech.* pp. 307–311.

TATSUMI, T. 1957 The theory of decay process of incompressible isotropic turbulence. *Proc. Roy. Soc.* A **239**, 16–45.

TATSUMI, T. 1960 Energy spectra in magneto-fluid dynamic turbulence. *Rev. Mod. Phys.* **32**, 807–812.

UBEROI, M. S. 1953 Quadruple velocity correlations and pressure fluctuations in homogeneous turbulence. *J. Aero. Sci.* **20**, 197–204 (corrigendum **21** (1954), 142).

UBEROI, M. S. 1963 Energy transfer in isotropic turbulence. *Phys. Fluids* **6**, 1048–1056.

VAN ATTA, C. W. & CHEN, W. Y. 1968 Correlation measurements in grid turbulence using digital harmonic analysis. *J. Fluid Mech.* **34**, 497–515.

VAN ATTA, C. W. & CHEN, W. Y. 1969 Correlation measurements in turbulence using digital Fourier analysis. *Phys. Fluids Suppl.* **12**, II 264–269.

VAN ATTA, C. W. & YEH, T. T. 1970 Some measurements of multi-point time correlations in grid turbulence. *J. Fluid Mech.* **41**, 169–178.

WYNGAARD, J. C. & PAO, Y. H. 1972 Some measurements of the fine structure of large Reynolds number turbulence. In *Statistical Models and Turbulence. Lecture Notes in Physics*, vol. 12 (ed. M. Rosenblatt & C. Van Atta), pp. 384–401. Springer.